List of Changes

We would like to thank both referees for their comments, which helped us improving the manuscript.

In summary, following the suggestions of referees, we
- Expanded the model description (Section 2.1 and Appendix B1)
- Better explained the riverine and atmospheric forcing (Sections 2.2 and 3.1)
- Renewed:
    o Fig. 3: included the climatological time series
    o Figs. 7, 14: used more suitable color schemes
    o Figs. 10-13: re-organized the panels for better visibility
    o Fig: 15: re-organized the panels and enhanced the quiver plots
- Introduced a new discussion section '4.3 Model limitations and perspectives', which:
    o Includes two new paragraphs
    o Two old paragraphs which was previously in Section 4.1
- Thoroughly corrected and clarified the text, where necessary.

Our point-to-point responses, and a marked-up manuscript version can be found below.

On behalf of all authors,
Onur Kerimoglu

Response to Anonymous Referee #1

Below, referee comments (starting with 'Comment'), and our specific responses (starting with 'Response' and/or [envisioned] 'Change') are provided in black and blue fonts, respectively.

Manuscript overview
The manuscript provides a model study into a particular flooding event in Northern Germany in order to determine the driving forces with regard to the marine response (German Bight area) to the event. To this end a slightly altered model is presented and applied under 2012 and 2013 conditions, plus 3 scenarios for 2013 to test the different, expected driving forces (meteorology, riverine input and a particular, 2 months long wind regime). The authors first show the anomalous forcing events, followed by plenty of model validation results and finally the model study into the expected drivers, for which they analyse the abiotic and biotic response of the system. They then conclude that the marine response to the flooding event was determined by both the enhanced riverine input (fresh water, nutrients, inner German Bight) and the anomalous meteorology of 2013 (outer German Bight) interacting with each other to alter the estuarine circulation patterns within the area.
The appendix contains detailed information about changes to the hydrodynamic and biogeochemical model, including applied equations and parameter values. It also contains some more validation results to justify some of the changes made to the model.

Review overview
In all, I'm quite charmed by the paper's objective and presented model study, with the specific aim (rather than a hypothesis) to determine which factors led to the marine reaction to a particular land-based event. The approach is valid and very interesting from a physical point of view.
Response: We thank the referee for the thorough review and positive remarks.

But I miss a good spatial validation of the model (surely the data in Figure 5 can provide that) which would more clearly quantify the problems in simulating the near shore environment.
Response: The data used for Figure 5 does not provide a homogeneous or balanced spatio-temporal representation within the study area, therefore it does not allow a reliable spatial validation suggested by the referee (see our response to the detailed comment below). However, we are convinced that the provided comparisons of modeled estimates against data from continuous Ferrybox measurements (Fig. 7 and A1), 3 stations for physical variables (Fig. 6), and 7 stations for biological variables (Fig. 8-9, 3 of these in Fig. 9 being near-shore stations in the study area) provide sufficient evidence that the model satisfactorily captures the spatio-temporal variability in the study area relevant for the purposes of the study. Therefore, we believe that the presented model performance assessment is sufficient for the purposes of the current study and a more detailed examination of the nearshore variabilities is beyond the scope of this manuscript (see also the responses below to the respective detailed comments).

Also, I'm not quite sure why a new model is presented which doesn't include bacteria in a study that aims to understand dissolved oxygen issues in the area. Why not use ECOHAM for that? Or better, a model with benthos included? The authors build on earlier work, and explicitly state that they use a simplified version of ECOHAM from which carbonate and bacterial dynamics have been eliminated (line 484, the geochemical model). They base

their new biogeochemical model (does it have a name?) on a previous model by the lead author that included mixothrophs, but these are not in here. So we have a biogeochemical model with just 2 phytoplankton species, 2 zooplankton species, fixed nutrient ratios inside zooplankton (the regulated uptake described in B1), no bacteria and no benthos. Isn't that just a stripped version of ECOHAM? Why not use that model? And if an important feature has been added (e.g. variable N,P ratio within phytoplankton), why not add it to ECOHAM?

Response: Some of these questions are suggestive of a number of misunderstandings, possibly led by ambiguities in the model description, which we hope to clarify in the following:

1) It is not entirely clear to us, what is meant by 'why not use ECOHAM for that'. If it means directly applying a readily available ECOHAM setup, this was not an option: to the best of our knowledge, the only available HAMSOM-ECOHAM setup, performance of which have been sufficiently documented (e.g., Große, 2017), is simply too coarse (20 km horizontal resolution, and 7 z-levels within the deepest part of the study area) for being able to capture the meso-scale features of the system, in particular, the haline stratification caused by the Elbe river (Pätsch et al., 2017).

2) If what the referee means is to couple ECOHAM with our GETM setup, which was previously identified to successfully reproduce the hydrodynamics of the study system (Kerimoglu et al., 2017a, Nasermoaddeli et al., 2018), this was not an option either: there is no ECOHAM code that can be readily coupled with GETM.

3) In this study, for the hydrodynamics, we used the GETM setup mentioned above. For the biogeochemistry, we used a model developed based on the earlier work of the first author (Kerimoglu et al., 2017b). In this model, description of the non-planktonic processes (i.e, production and destruction of detritus, oxygen consumption processes, benthic remineralization) were adjusted to the study system by adopting almost the same structure and descriptions provided by ECOHAM. It should be noted that, given that the present model accounts for the variable stoichiometry and chlorophylll content of phytoplankton, adopting the descriptions of plankton growth and interactions from ECOHAM as well would mean a backwards step, technically.

4) In the original ECOHAM model, 'bacterial' oxygen consumption occurs in proportion to the DOM breakdown. In our model, although the bacterial biomass is not explicitly considered, the oxygen consumption in proportion to DOM breakdown is represented. The only difference between the two approaches is that in ECOHAM bacterial abundance is potentially limiting for the DOM breakdown rate, while in ours, it is not (see the detailed response below).

5) It was again not entirely clear to us what is exactly meant by 'a model with benthos' by the referee. To clarify, our model does comprise a benthic module that describes the aerobic and anaerobic early diagenesis in the sediment, exactly as described by ECOHAM. We acknowledge, however that the descriptions of benthic processes provided by this model are simplistic, and potentially responsible for, e.g., inaccuracies in oxygen consumption rates (see below).

6) Although the description of the non-planktonic processes are similar, differences in the descriptions of plankton growth and interactions between our model and ECOHAM are significant. Therefore, referring to our model as 'a stripped version of ECOHAM' would be misleading.

I would also argue there are more complex models out there better suited for a dynamic, shallow area like the German Bight, particularly for a study involving nutrient concentrations and bottom oxygen conditions.

Response: There are certainly more complex models, but considering the purposes of our study, it is not clear in which specific sense would such a model be better suited. It should be noted that, with regard to benthic/pelagic coupling, models of similar complexity have

been used until recently, for studying the nutrient concentrations and bottom oxygen conditions in the North Sea (e.g., Große et al., 2017, using ECOHAM), as well as other similarly dynamic coastal shelf systems such as the Louisiana Shelf (e.g., Fennel and Laurent, 2018) or even shallower systems such as the Chesapeake Bay (Irby et al. 2018).

Given the lack of validation with Chla observations (the only station in the area of interest shows a normalized model bias of 1.12)
Response: the comparison of estimated chlorophyll concentrations with the data from four stations does build confidence in the simulated chlorophyll in the study area: although three of these stations are outside the exact study area, they are still close enough to be representative, as they are characterized by a similar abiotic environment that is typically found in the study area. Although a normalized bias of 1.12 for chlorophyll is obviously not very good (which we openly highlighted and discussed in the manuscript), it is not alarming, considering that chlorophyll is governed by exponential growth dynamics, and therefore commonly shown (when shown at all) in logarithmic scale in model-data comparison plots.

and benthic nutrient concentrations
Response: necessity for the presentation of a validation of benthic nutrient concentrations of fluxes (which is very rarely done in studies similar to ours) is not clear.

my confidence in the biogeochemical model results is not large.
Response: as a clarification, we do not claim confidence in the predictions of our model in an absolute sense, and providing such precise predictions is not our purpose in this study either. However, we are confident that the model is useful in gaining insight into the overall response of the ecosystem to changes in hydro-meteorological conditions, which is the purpose of this study (see also our response to point 3 below).

Although the authors are in parts clear about the model limitations, they should add text on 1. Their choice of biogeochemical model, 2. What makes it better suited here than ECOHAM,
Response: Although all technical details extensively listed above are not likely to be relevant for the audience, some clarification of the model design and a discussion of potential future development will serve to improve the general model description.
Change: we extended the model description sections (2.1 and B2.1) to describe more clearly what was taken from ECOHAM and what was not. We also included two new paragraphs in the new discussion section 4.3, on the similarities with and differences from other models, as well as potential future development and applications. At the publication stage, we will also store the model code in a public repository and provide it in the 'Code and data availability' section, so that anyone interested can inspect and use the code.

3. More Chla validation and
Response: we are convinced that the presented validation is already plenty, targeted, and based on an extraordinarily rich dataset.
Change: in line with our view explained above, we stressed in the Discussion (section 4.1) that our NPPR estimates should be interpreted in terms of system response to hydro-meteorological forcing, and not as predictions in an absolute sense.

4. The role the sediments play in nutrient dynamics in shallow areas.
Response: this suggestion is potentially caused by a misunderstanding that our model does not have at all a benthic module (see above). We acknowledge, however, that some complex benthic dynamics, such as the spatial heterogeneities in sediment fluxes driven

by sediment permeability are not captured by our simple model, which is potentially responsible for inaccuracies, e.g., in oxygen consumption rates.
Change: we included a discussion of these effects.

Or, as an alternative, the authors could limit their analysis to the physical part, which is quite strong in the manuscript and would allow for a better focus of the text: there is enough to analyse there as shown by the authors, and the conclusions would not change.
Response: Referee's suggestion of limiting our analysis to the physics alone, will invalidate roughly half of our conclusions, and hence substantially reduce the scope and significance of our study. We would therefore prefer to keep the analysis regarding the biogeochemical processes. Please see below our responses to the specific comments.

Recommendation
Major revision

Detailed Comments
L 56-57: One cannot expect that the marine transport of riverine inputs is purely dependent on the inter-annual variability in the river discharges. In any marine area the meteorological conditions (mainly wind and temperature) will play a large part in the transport, as will alongshore currents. Then there are influences like mixing by ships, the presence of off-shore wind farms, and further-afield influences like the Rhine discharge. So I thought this sentence a little odd.
Response: We do not think that the sentence referred by the referee ('The extent to which the hydrodynamical structure, and the transport of riverine material within the German Bight depends on the inter-annual variability in riverine discharges is not fully understood.'), implies that 'the marine transport of riverine inputs is purely dependent on the inter-annual variability in the river discharges'. The emphasis here is on the not fully understood '*extent*', i.e., the magnitude and scope of this dependency.

Fig. 2: The diagram is clear until one gets to the appendices, where it is stated that phytoplankton exudates DOM (L463), that zooplankton excrete into the DIM pool (L466) and the unassimilated fraction ingested by zooplankton becomes DOM (L486). None of this is visible in the model diagram, as all functional groups just exude large detritus ... ?
Response: The mentioned links were intentionally neglected in an attempt to make the diagram easier to understand.
Change: the simplifications were clarified in the caption of Fig. 2 and the reader is referred to Appendix B for a detailed model description.

L 101: The authors state here that the underwater light conditions are determined by detritus, DOM and a background value representing SPM. But in section B2.2 they state that phytoplankton is also included in the light calculation. Please make this consistent.
Change: shading caused by phytoplankton is now mentioned in the sentence.

L 116: Please provide the website for the atmospheric deposition fields.
Response: The website is provided in the 'Code and data availability' section. (L401), along with a number of other data sources. We do not think that duplicate listing of these sources in the main text is necessary.

L 117: Please state which rivers were included within the Wadden Sea area. Just major ones (Elbe, Weser, Ems, ...) or also local Dutch and German rivers like the Accumersiel, Bensersiel, Wangersiel, Miele, etc.? I know from experience that these rivers are also part of the mentioned database, which I think is called the OSPAR ICG-EMO riverine database.

So I would assume they were used, but this needs to be stated clearly.
Response: in this study, we only used the discharges from major rivers shown in Fig. 1. Previously, we had observed that inclusion of small rivers did not make an appreciable difference in the present setup.
Change: it was mentioned here that the dataset is indeed called OSPAR ICG-EMO riverine database, and that we considered only the major rivers as shown in Fig. 1.

L 124: "a 3600 s time window", why not say 1 hour time window? In the caption of Figure 4 the authors mention an hourly resolution, not a 3600 s one.
Response: 3600s is how it is specified from a drop-down list in the web-interface of the cosyna data portal, which we thought could have been relevant.
Change: we now use 'hourly' for the sake of consistency.

L 134: Again, a website for the ICES data should be provided.
Response: The website was already provided in the 'Code and data availability' section.

L 139: This section is called Results, but quite a large part of it is model validation results. I would like to see this separate from the forcings analysis (section 3.3 onwards), and would therefore call this section "Model validation" and rename section 3.3 to be section 4 "Results".
Response: The material we present in 3.2 is not a model validation without context, but it is partially targeted towards assessing the ability of the model to capture the flood event specifically (Fig.7,9, and partially Fig.6). Therefore it is important that this section follows the 'Hydrological and Meteorological Conditions' section, which are also clearly part of the Results. It is not clear, what the benefit of separating section 3.2 from the rest of the results would be. Therefore, we would prefer to keep the structure of the manuscript as it is, which we believe to be well connected and easy to follow.

L 144: Naturally the nutrient loads follow the flow peak, but what about concentrations? If we assume heavy rainfall caused more run-off then nitrogen concentrations may stay the same, but phosphorous concentrations (usually from sewage treatment works) may be diluted. So please provide some measure of the changes in concentrations for these rivers.
Response: we checked the seasonal variations in concentrations., but have not found any systematic or considerable variations coinciding with the flood event (as now mentioned in Section 3.1) that requires an extensive discussion. We conclude therefore that the fluxes are driven by the increased discharge rates, which is also now explicitly stated.

Fig. 3: The Ems does not show the flood peak found in the Weser and the Elbe, suggesting it was a local event. Nevertheless I would like to see results for the Rhine/Meuse system, which will influence the area of interest here under normal conditions.
Response: it was mentioned in the text (L.141-143) that the flood event was caused by an event over central Europe, that affected the basins of Elbe and Weser rivers. However, it is indeed not clear from this explanation, whether other rivers may have been affected or not.
Change: we analyzed all rivers considered and found no such extreme events as in Elbe and Weser. This is now indicated in Section 3.1.

L. 146-150: Please provide some information on whether 2012 was in any way an average year or not.
Change: we now included decadal averages in the Figure, which shows that 2012 is indeed an average year, which we mention in Section 3.1.

Fig. 4: It seems that 2013 is characterized by mainly eastern winds all the way up to June. So why were only the June-August winds selected for a scenario? Because they do not seem easterly much in that period. The winter and spring easterlies are now part of the M12 scenario, together with the different temperature record etc.

Response: the point we aim to make with W12 scenario is that the short term wind forcing is so important for the system that the wind forcing only during summer, regardless of the earlier forcing (including wind direction), can make many patterns (especially stratification) resemble those in 2012 (e.g., L.205-206, L.215-220, L.340). Including a longer time period would erode the strength of the scenario by bringing in additional complexities.

Fig.5 : Please make this a colour graphs, the gray scales are very hard to distinguish from one another. And why is count on the colour bar at all? I assume this is the number of observations in a given point throughout the year? But why not use three different colours for the three years instead?

Response: these plots are two-dimensional histograms, where counts represent the frequency of observation-simulation pairs. Higher count (darker shades) simply indicates higher density of pairs, which does not need an exact perception.

Change: we now clarify in the caption that these are two-dimensional histograms, and that counts represent the occurrence frequency of simulation-observation pairs.

Fig. 5: And as said before, I would really like to see a spatial validation graph, which would provide more detail on the nearshore errors in the model. I realise there are quite a large number of figures already in this manuscript, but would suggest some could be put in the appendix, e.g. Figure 6 and Figure 8 (which shows 3 stations which are in the model domain but not in the area of interest, and which therefore do not provide much context for the described work).

Response: Both Fig. 6 and Fig. 8 are essential for the manuscript. All 3 stations in Fig. 6 are within the study domain and show that the model mostly accurately reproduced the measured temperatures and salinities. Although the three stations in Fig. 8 is not within the area of interest, they are quite close and constrained by an abiotic environment (resource abundances, water depth, meteorological and physical conditions) similar to that in the study area, therefore they help building confidence in the biogeochemical model within the study area. In fact, by demonstrating that the model is able to reproduce the baseline levels of measurements obtained at different stations, these plots serve in gaining insight into the model's skill in reproducing cross-shore gradients, which is what the referee probably wants to see with the 'spatial validation graph'. Finally, Fig. 9, which shows the modelled and measured nutrient concentrations at stations located along the coastline downstream of the mouth of Elbe, serves in evaluating the skill of the model in reproducing the spatial distribution of nutrients following the flood event. We are therefore convinced that the presented analyses provide an extraordinarily good basis for the assessment of the performance of the model and provide evidence for its suitability for the purposes of this study.

L162: Why use Kelvin here when Fig. 4 uses Celsius?

Response: In Fig.4, the context is absolute air temperature, where Celsius is an arguably more convenient scale than Kelvin. In the context of a temperature difference Kelvin is practically identical to Celsius but Celsius may indeed be familiar for the general audience.

Change: we replaced K with Celsius in the text.

L175: The authors state that the plume was realistically reproduced as the sharp increase in NO3 al Helgoland was captured. But this is not very clear from Fig. 8, rather that 2

observed peaks in DIN are not reproduced by the model and one peak is slightly reproduced. So I'm not convinced that the plume is simulated realistically, just from this figure.

Response: for convenience, we show in Fig. R1-1 below an enlarged and annotated version of the related panel in Fig.8 of our manuscript. As can be more clearly seen here, the distinctive 'sharp increase in DIN during June/July 2013' (as stated in L.175) is indeed realistically captured by the model (please see also the Fig. R2-1 included in our response to Referee #2 regarding a related comment, where we show that the ability of the model to capture the DIN peak after the flood is closely coupled with the ability of the model in capturing the freshwater plume of the flood).

Change: we expanded on this sentence and spelled out our take on this particular result.
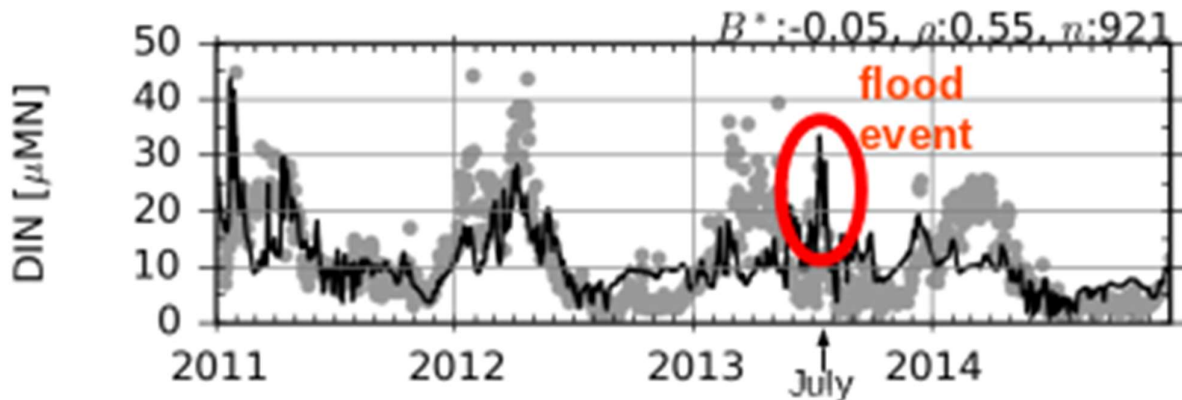
Figure R1-1: DIN Concentrations measured (gray dots) and modelled (black line) at the Helgoland station (modified from Fig. 8 in the manuscript).

L177: why do the authors have such a high Si value on the western boundary? Is this an artefact of the simulation that generated the boundary conditions?

Response: as explained in L.176-178, overestimated Si values are indeed caused by the fluxes from the western open boundary, which is due to too high concentrations specified as the boundary conditions.

Change: we specified that this is caused by the available data used to specify the boundary conditions.

L181: The model fails to get the spring bloom timing right. I would say: use a different model or just focus on the physics. The Chla comparison for Helgoland is quite bad and this is the only station presented here for validation of Chla in the area of interest. Does ICES have more Chla data in the specific area?

Response: In our view the immense effort of changing the biogeochemical model is not justified for the scope of the present study. Focusing only on physics would mean removal of roughly a half of the presented material, which we consider to be relevant and useful. Opting for any of these paths would require very substantial reasons for doing so, which we do not see.

1) The model indeed fails to capture the timing of the spring bloom at Helgoland, as was mentioned in the L.181 of the manuscript, however this is not directly relevant to the subject matter of the manuscript.

2) We disagree that the model comparison in Helgoland is 'bad', when put in the right context: we are not aware of any other model that shows better performance at this particular station.

3) Comparison at other stations build confidence in model results, even if they are not directly in the area of interest. As mentioned above, these comparisons show that the

higher concentrations at the coastal stations and lower concentrations at the off-shore stations are reproduced, which can be expected to hold within the study area.
4) Our biogeochemical model offers many other useful insights into other variables such as nutrient and oxygen concentrations, which are all essential for the manuscript.
5) We acknowledge that the relatively poorer model performance regarding chlorophyll (relative to the other variables), requires a more careful interpretation of directly relevant model results, such as the primary production estimates.
6) ICES dataset offers chlorophyll measurements, however, as shown in Fig. R1-2 below, the spatio-temporal distribution of the reliable (having consistent metadata) data available within the study area is so heterogeneous, that, a construction of, for instance a 'summer average' map with the data will be heavily influenced by the sampling frequency in time and space. Therefore it is not straightforward to achieve a consistent validation with this data set.
Change: Per point 5 in our response above, we stressed in the discussion (section 4.1) that the NPPR estimates, which are directly related with overestimated chlorophyll values, need to be interpreted with care. In particular, we stated that the absolute magnitudes may be misleading, but that the response of NPPR to the hydro-meteorological conditions can serve in understanding the behavior of the system.
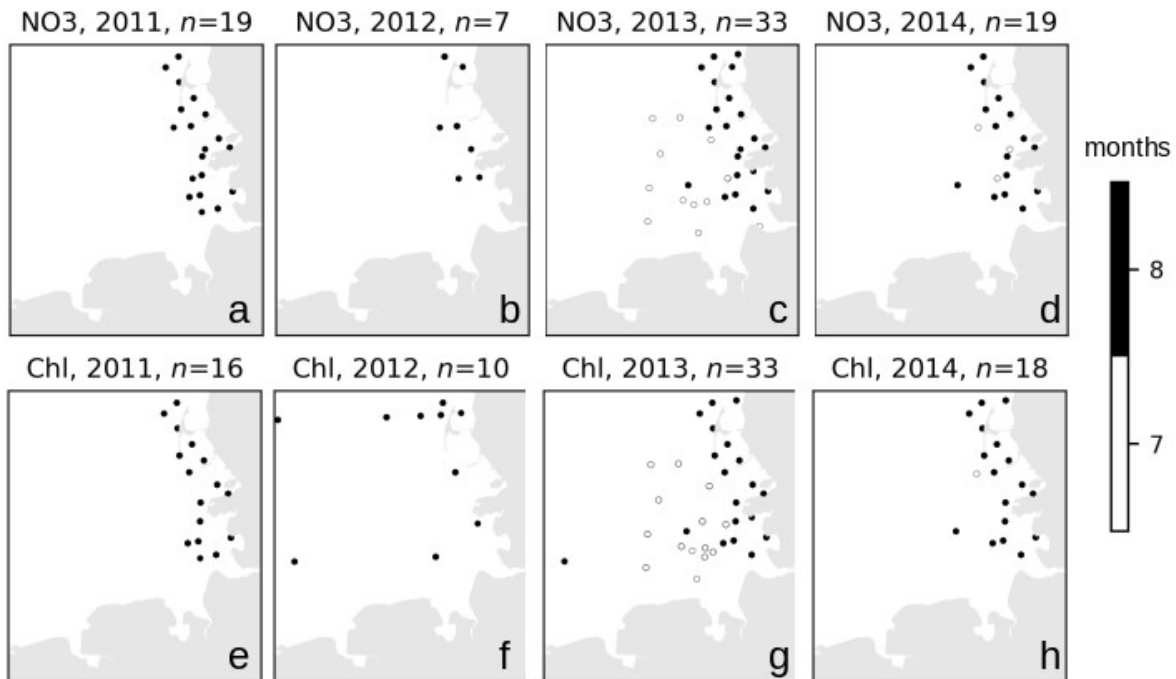
Figure R1-2: Spatial distribution of reliable chlorophyll measurements in the ICES dataset during July and August for each simulation year. n is the number of unique locations (identified by latitude-longitude pairs rounded to nearest 0.05º).

Fig 10: This figure, and also figures 11 and 12 are too small for readers to easily read. I would suggest that the graph itself is made larger in the manuscript but also that the colour bar is changes to one large one on each side (one for S, one for T), so the graph becomes more accessible. These graphs are the essential results presented in the manuscript, so please do them justice.
Response: the particular suggestion of the referee can indeed be applied to Fig. 10, but not equally well to Fig. 11 and not at all to Fig. 12, as in the latter, not only two, but four variables need to be shown. We do not think that presenting these figures with different layouts will improve the manuscript. Considering that the latitude and longitudes are

presented in larger form in Fig. 1, these labels can be removed to save space for larger colorbars. When these Figures are printed in full page width in the final publication, the text will be presumably easier to read as well: for the discussion paper, they are constrained to 12cm width, as was suggested by the style guidelines.
Change: The panels were enlarged by removing latitude and longitude labels except those at the margins, and moving the colorbars in horizontal orientation, and enlarged form, to the top of each column in Figures 10-13.

L223: It is not clear to me why increased stability should have a direct effect on the underwater light penetration, particularly as SPM dynamics are just a background value. Are the authors referring here to limited nutrient exchange and thus less bioshading? They do for the OGB, but in the CGB the flood causes increased stratification and brings in nutrients, resulting in more primary production,. On L246 it is simply stated that increased stratification enhanced the underwater light regime within the CGB. Please explain and provide a reference. Are you referring to increased remineralization within the euphotic zone? I would also like to see some evidence of the underwater light response in the simulations.
Response: we would like to clarify that in this sentence ('intensity of the thermohaline stratification, [and hence], gives insight into the average light conditions primary producers experience in the deeper zones') there was a typo: 'deeper' should be in fact 'surface'. As it may now have become clear after this correction, with this sentence, we were not referring to the changes in the 'underwater light penetration', but simply to the obvious fact that, due to the reduced vertical mixing, phytoplankton growing at the surface layers can stay there longer, enhancing therefore the 'light conditions [they] experience'. Due to the large uncertainties in the underwater light climate, and only the partial coverage of its response to the hydroclimatological factors (e.g., see L.359-361 in Discussion), we would not like to present potentially misleading estimates.
Change: 'deeper zones' in the sentence was replaced with 'surface layers'.

L248: Please introduce figure 13 first and explain the DO abbreviations before going into the analysis.
Change:done.

Fig. 6: Can the authors speculate why their biogeochemical model is unable to quantitatively reproduce the observed oxygen minimum? What processes do they think the model misses?
Response: We believe that the insufficient oxygen depletion as suggested by Fig. 14 (probably this the one the referee is referring to, and not Fig. 6) might be associated with the inaccuracies in benthic consumption rates. A model that considers the horizontal heterogeneities in the soil permeability, and that dynamically calculates the vertical profiles in the benthic layer could potentially better reproduce the oxygen consumption rates. In order to prevent any potential misunderstanding (see our response to the 'Review overview' above) we would like to clarify once again, that the model does have a benthic component based on the benthic model of ECOHAM. This is however a simple model that dynamically tracks the nutrient and carbon pools only, and the benthic DO consumption rate is computed based on a linear relationship with benthic remineralization, based on empirical evidence (see Paetsch and Kühn 2008).
Change: we have included a discussion along this line in the text.

Fig. 15: These again are too small and I cannot see the arrows at all in the difference figures.
Change: we added outlines to the arrows, removed unimportant details and reorganized

the panels for better visibility.

L282: Yes, they do but this is rather an open door. Any reader would have expected that from the start, and would have been surprised if this was not the case.
Response: that 'the efficiency of estuarine circulation is determined by an interplay between the meteorological and hydrological conditions' may be an intuitive expectation, but we are not aware of any previous study that provided evidence to support this intuition. Nevertheless, the word 'indicate' potentially implies 'novelty', which was not intentional.
Change: we reformulated and clarified the sentence.

Sec4: Please discuss the lack of bacterial dynamics in the discussion, and the effect this can have on the simulated results.
Response: we would like to clarify that, although the presented model does not account for the bacteria biomass, the primary function of bacteria in the context of the current study, at least as represented in biogeochemical models (such as ECOHAM), i.e., decomposition of DOM and the resulting DO consumption (probably this is what concerns the referee, based on their comment under 'Review overview') is represented in our model by a first order kinetic term (Fig. 2, Table B9). Conceptually, this is equivalent to assuming that the degradation of DOM is not limited by bacterial biomass. We are not aware of any evidence against this assumption for the study area. For the case of Lake Kinneret, Li et al. (2014) have shown that the DO estimates of a model version similar to ours, that also does not explicitly describe bacterial biomass 'were not significantly different' than those estimated by two other model variants where bacterial dynamics were explicitly described. In conclusion, we do not see the need for an extensive discussion of the lack of an explicit description of bacterial dynamics.
Change: we removed the potentially misleading part of the sentence in Section 3.1 (exclusion of bacterial dynamics), and explained instead how DOM remineralisation is simplified in comparison to the original model.

L312: I would say the model was able to reproduce the physical characteristic features of the system quite well.
Response: we believe we provide evidence for the ability of model to reproduce several non-physical characteristic features of the system as well.

L316: "The skill of the model ... is notable", quite a nice notation as it is meaningless. Notable means it can be noted, it says nothing about it being good or bad.
Change: we expanded this in relation to Helgoland being at a transition zone, and that the reproduction of certain signals, such as the summer peak in DIN being dependent on reproduction of the spread of the freshwater plume.

L320-333: I'm not sure why this is include here, this is not of interest for the general reader I would think. Therefore I would put this in an appendix at most.
Response: we believe that a part of this paragraph is necessary, as it provides a perspective in relation to the recent modeling studies, and points to the important trade-off between computational expense and performance. This is potentially relevantfor anyone who is interested in coupled physical-biogeochemical modeling.
Change: considering the length of the revised discussion, we removed the technical information in this paragraph, and to provide a better context, we moved it to the new discussion section 4.3.

L349: I fail to see the prolonged stratification in figure 11. As these are all July averages I don't see a time indication in this figure at all.

Change: the sentence was reformulated as 'uninterrupted phases of stratification during July, that gave rise to a large average density difference (Fig. 11), … '.

L385: I object to the use of the word "satisfactorily" when it comes to the reproduction of the biogeochemical features of the German Bight ecosystem.
Response: we are convinced that the coupled model system satisfactorily reproduces a number characteristic features of the ecosystem, that are relevant for the purposes of this study.

Table B5,B6,B8: If parameter values are provided then references on what these are based on should be included as well. Assuming these values have not been published before.
Change: provided the sources of parameters, where possible and necessary.

Language
In general I found the manuscript very readable, yet the English used was not always correct or as expected. I found several mistakes regarding single/plural (e.g. L 140, "the discharge rates ... peaks", L156 "Comparison ... are shown", L299 "potential sources of error needs to be addressed"), omissions of articles (e.g. L 156 A "Comparison of", L187 "Despite a tendency to overshoot, the range of", L205 The "Effect of exchanging", L211 "further to the North"), additions of articles in unnecessary places (e.g. L 143 "over the central Europe", LL232 "river forcing of the 2012 is used", L232 "the plume of the DIP") and omission of connecting words (e.g. L157 "are located at shallow sites, and therefore provide", L373 "the presence of regional differences"). I suggest the authors check their English thoroughly before the next submission. But I love the double negative found on L439: "leading to near-complete elimination of negative values of the total mixing being removed". So the removal has been eliminated?
Change: we eliminated the mistakes pointed out by the referee, carefully checked the text and corrected similar mistakes.

References

Fennel, K., Laurent, A. (2018) N and P as ultimate and proximate limiting nutrients in the northern Gulf of Mexico: implications for hypoxia reduction strategies. Biogeosciences 15, 3121–3131.

Große, F. (2017) The influence of nitrogen inputs on the oxygen dynamics of the North Sea. PhD Thesis, University of Hamburg. Pages 82-83.

Große, F., Kreus, M., Lenhart, H.-J., Pätsch, J., and Pohlmann, T. (2017) A Novel Modeling Approach to Quantify the Influence of Nitrogen Inputs on the Oxygen Dynamics of the North Sea, Frontiers in Marine Science, 4, 1–21.

Irby, ID., Friedrichs, M.A.M., Da, F., Hinson, K.E. (2018) The competing impacts of climate change and nutrient reductions on dissolved oxygen in Chesapeake Bay. Biogeosciences 15, 2649–2668.

Kerimoglu, O., Hofmeister, R., Maerz, J., Riethmüller, R., and Wirtz, K. W. (2017a) The acclimative biogeochemical model of the southern North Sea, Biogeosciences 14, 4499–4531.

Kerimoglu, O., Jacquet, S., Vinçon-Leite, B., Lemaire, B. J., Rimet, F., Soulignac, F., Trévisan, D., and Anneville, O. (2017b) Modelling the plankton groups of the deep, peri-alpine Lake Bourget, Ecological Modelling, 359, 415–433.

Li, Y., Gal, G., Makler-Pick, V., Waite, A. M., Bruce, L. C., and Hipsey, M.R. (2014) Examination of the role of the microbial loop in regulating lake nutrient stoichiometry and phytoplankton dynamics. Biogeosciences, 11, 2939–2960.

Nasermoaddeli, M. H., Lemmen, C., Stigge, G., Kerimoglu, O., Burchard, H., Klingbeil, K., Hofmeister, R., Kreus, M., Wirtz, K. W., and Kösters, F. (2018) A model study on the large-scale effect of macrofauna on the suspended sediment concentration in a shallow shelf sea, Estuarine, Coastal and Shelf Science 211, 62-76.

Pätsch, J., Kühn, W. (2008) Nitrogen and carbon cycling in the North Sea and exchange with the North Atlantic—A model study. Part I. Nitrogen budget and fluxes. Continental Shelf Research 28, 767-787.

Pätsch, J., Burchard, H., Dieterich, C., Gräwe, U., Gröger, M., Mathis, M., Kapitza, H., Bersch, M., Moll, A., Pohlmann, T., Su, J., Ho-Hagemann, H. T., Schulz, A., Elizalde, A., and Eden, C. (2017) An evaluation of the North Sea circulation in global and regional models relevant for ecosystem simulations, Ocean Modelling, 116, 70–95.

Response to Anonymous Referee #2

Below, referee comments (starting with 'Comment'), and our specific responses (starting with 'Response' and/or [envisioned] 'Change') are provided in black and blue fonts, respectively.

Comment: This study introduces a new biogeochemical model, consisting of modified versions of previously published models. Coupled with a hydrodynamic model with an improved mixing scheme, the system is validated in the German Bight region, and used to assess the impact of meteorology and river forcing on a specific flood event in 2013. The conclusion is that an interplay of the two resulted in anomalous conditions, as previously noted in observations.
The paper acts as both presentation and validation of a new modelling system, and an investigation into a specific event. While it could potentially work as separate papers, the paper is well enough written and laid out, and the validation both sufficiently comprehensive and targeted, that it works well and is an enjoyable and interesting read. I recommend publication in Biogeosciences subject to a few minor comments detailed below.
Response: We thank the referee for the careful read of the manuscript, positive assessment of our work and constructive suggestions.

The biogeochemical model appears to be a work in progress towards a different mixotroph-based model, rather than a model likely to be widely used in its present form, if I've got the correct impression? This is fine, given its structure seems sensible and plenty of validation is presented, but it would be worth adding some discussion about what sets it apart from other similar models, particularly ECOHAM, and what future developments are intended.
Response: The Referee's impression is correct, that the model presented in this study is intended to be developed further. Nevertheless, we also believe that at its present state, it can already serve the purposes of this study. We agree that further clarification and additional discussion of the model structure and future directions is needed.
Change: we clarified the similarities and differences of our model with similar models, particularly ECOHAM in the revised manuscript, and discussed the potential directions for further model development.

Given that it's central to the study, in Section 2.1 and/or 2.2 it would be worth explicitly detailing which variables are used in the atmospheric and riverine forcing, and how they're applied to the model (e.g. bulk formulae? are rivers applied just at the surface or over the full depth?).
Change: further details on the application of meteorological and riverine forcing in the model were provided in section 2.2. A reference in this section was moved to the more relevant section 3.1.

"using the 'spatial.cKDTree' package from the Scipy library of Python 3.5." – add the Scipy version number for completeness.
Change: the Scipy version used for the revised manuscript is now provided.

Figure 3 shows the Ems, and that this doesn't have anomalous discharge in 2013. This isn't mentioned or discussed in Section 3.1, and should be. Also, the "dashed blue lines" appear solid.
Change: we mentioned which rivers were affected and which were not in Section 3.1, and

corrected the caption of Fig. 3 (which now includes the 2005-2014 climatology, shown with dashed lines).

"Simulated temperature and salinities . . . (Fig. 5) . . . exhibit no signs of systematic deviations or biases." The calculated B* values are near-zero, but by eye it looks like there's a cold bias, particularly at colder temperatures, and that salinity is usually too high. Is this just a trick of the eye, or are the simulated and observed distributions different? Please also state what B*, rho and n are in the caption of Fig. 5, as per Fig. 6.

Response: A careful assessment of the figure reveals that a slight cold bias at the lower range is indeed present, which seems to be canceled out by the slight warm bias at the higher range. But these deviations are mostly within a 1K range, therefore presumably do not have a significant effect. At an intermediate range, salinity is somewhat (in the order of 2 g/kg) overestimated, indicating insufficient spread of coastal waters with low salinity. This may either be due to (still) underestimated horizontal mixing, or inaccuracies in the advection patterns. Either way, the potentially underestimated salinity during the studied event may lead to an underestimation of the importance of riverine discharges on the stratification dynamics in the transition zone characterized by intermediate (29-32 g/kg) salinities.

Change: a more nuanced description of the model performance was provided in the paragraph describing Fig.5 (section 3.2), and implications thereof were provided in the discussion (section 4.1). Definition of B*, rho and n were included in caption of Fig.5.

"(Fig.8) . . . The ability of the model to capture the sharp increase in DIN during June/July 2013 at the Helgoland station suggests that the spreading of the plume of the Elbe-Weser rivers following the flood event was realistically reproduced." The model completely misses the peak earlier in the year, and also in early 2014. Can you be confident therefore that this result was obtained for the right reasons?

Response: The sentence was indeed misleading, as the word 'suggest' emphasizes the uncertainties of mechanisms causing the summer peak. The reasons for not reproducing the peaks in DIN during winters are not clear, but the reason for the mid-July peak as captured by the model is very likely to be the flood. Occurrence of such a high summer DIN peak at this station is not common under typical hydrological settings. In this particular case, we can tell with certainty that the reason for the model to produce such a high summer peak is the flood: the Figure R2-1 below shows how the flood water characterized by low-salinity and high DIN move within the 45 days after the flood event. These findings are consistent with the *in-situ* data shown by Voynova et al. (2017, Fig. 12), building confidence to believe that the unique DIN peak measured at Helgoland in July 2013 was caused by the flood in reality as well.

Change: the figure shown below would be too specific for the manuscript, but this finding was more clearly described in discussion.
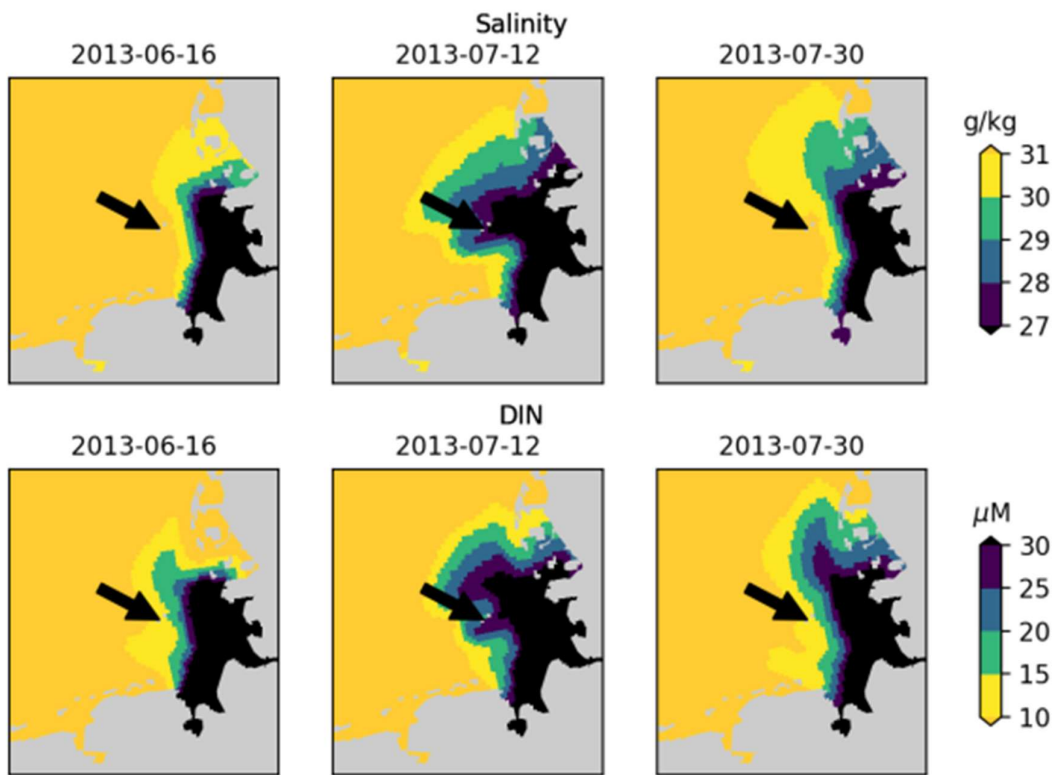
Figure 2-1: Salinity and DIN concentrations following the flood event. Arrow shows the location of monitoring station at Helgolands.

In Fig. 7, plotting the average in white is confusing – I initially thought there were separate yellow/blue lines either side of it, and the white was blank space. Plotting it in dark yellow/blue might be better. Also, make clear in the caption that the line indicates the average and the shading the standard deviation (I assume this is the case?).
Change: dark yellow/blue lines are now used to show the averages, and it is clarified that the dark lines indicate averages and shades indicate standard deviations (indeed).

In Fig. 14 it would be best to avoid plotting red and green together, as this renders it inaccessible to those who are red-green colour blind. (Disclaimer: I'm not colour blind myself, so can't say for sure.)
Change: a colorblind-friendly palette is now used in Fig.14.

References

Voynova, Y. G., Brix, H., Petersen, W., Weigelt-Krenz, S., and Scharfe, M. (2017) Extreme Flood Impact on Estuarine and Coastal Biogeochemistry: the 2013 Elbe Flood, Biogeosciences, 14, 541–557.

Interactive impacts of meteorological and hydrological conditions on the physical and biogeochemical structure of a coastal system

Onur Kerimoglu[1,2], Yoana G. Voynova[1], Fatemeh Chegini[3,4], Holger Brix[1], Ulrich Callies[1], Richard Hofmeister[1], Knut Klingbeil[3], Corinna Schrum[1], and Justus E.E. van Beusekom[1]

[1]Institute for Coastal Research, Helmholtz-Zentrum Geesthacht, Germany
[2]Institute for Chemistry and Biology of the Marine Environment, Carl von Ossietzky University Oldenburg, Germany
[3]Leibniz Institute for Baltic Sea Research, Warnemünde, Germany
[4]now at: Max Planck Institute for Meteorology, Hamburg, Germany

Correspondence: Onur Kerimoglu (kerimoglu.o@gmail.com)

Abstract. The German Bight was exposed to record high riverine discharges in June 2013, as a result of flooding of the Elbe and Weser rivers. Several anomalous observations suggested that the hydrodynamical and ~~the biogeochemical state~~ biogeochemical states of the system ~~was~~ were impacted by this event. In this study, we developed a biogeochemical model and coupled it with a previously introduced high resolution hydrodynamical model of the southern North Sea, in order to better characterize these impacts, and gain insight into the underlying processes. Performance of the model was assessed using an extensive set of *in-situ* measurements for the period 2011-2014. We first improved the realism of the hydrodynamic model with regard to the representation of cross-shore gradients, mainly through inclusion of flow-dependent horizontal mixing. Among other characteristic features of the system, the coupled model system can reproduce the low salinities, high nutrient concentrations and low oxygen concentrations in the bottom layers observed within the German Bight following the flood event. Through a scenario analysis, we examined the sensitivity of the patterns observed during July 2013 to the hydrological and meteorological forcing in isolation. Within the region of freshwater influence (ROFI) of the Elbe-Weser rivers, the flood event clearly dominated the changes in salinity and nutrient concentrations, as expected. However, our findings point out to the relevance of the peculiarities in the meteorological conditions in 2013 as well: a combination of low wind speeds, warm air temperatures and cold bottom water temperatures resulted in a strong thermal stratification in the outer regions, and limited vertical nutrient transport to the surface layers. Within the central region, the thermal and haline dynamics interactively resulted in an intense density stratification. This intense stratification, in turn, led to enhanced primary production within the central region enriched by nutrients due to the flood, but reduction within the nutrient-limited outer region, and it caused a wide-spread oxygen depletion in bottom waters. Our results further point to the enhancement of the current velocities at the surface as a result of haline stratification, and intensification of the thermohaline estuarine-like circulation at the Wadden Sea, both driven by the flood event.

1 Introduction

Riverine discharges influence the thermohaline stratification, nutrient availability and as a result, primary production within the coastal zones (e.g., Hickey et al., 2010; Cloern et al., 2014; Emeis et al., 2015). Excess amounts of riverine nutrient inputs cause coastal eutrophication, associated with a host of problems (Smith and Schindler, 2009), including development of dense
25 and harmful algal blooms (e.g., Garnier et al., 2019), decline of submerged vegetation (e.g., Dolch et al., 2013), and oxygen depletion (see the review by Fennel and Testa, 2019). Fraction of riverine freshwater and nutrients that reaches the open ocean is an open question, with estimates ranging between 15% and 80 % (Sharples et al., 2017; Izett and Fennel, 2018).

Mixing of riverine freshwater with the surrounding saline marine waters at the coasts is driven by a set of hydrodynamical processes intriguingly linked together (for a recent review, see Geyer and Maccready, 2014). The freshwater inputs by rivers
30 may lead to haline stratification in the coastal region, in the absence of any thermal stratification (van Aken, 1986). Horizontal density gradients caused by riverine freshwater inputs govern gravitational circulation (i.e., exchange flow), where the seaward flow of the lighter water at the surface is counteracted by a landward flow of the saltier, denser waters near the sea floor (see Burchard et al., 2018). Destabilizing and stabilizing effects of flood and ebb currents, respectively, may further enhance the gravitational circulation (Burchard and Hetland, 2010).

35 The study system, the German Bight, is a shallow area located in the southeastern North Sea (Fig. 1). The prevailing wind direction is southwesterly (Siegismund and Schrum, 2001), governing a large cyclonic gyre within the southern North Sea (Sündermann and Pohlmann, 2011). But under easterly and northeasterly winds, anticyclonic circulation may prevail (Becker et al., 1992; Dippner, 1993; Callies et al., 2017). Occurrence of thermohaline stratification within the German Bight is driven by the the buoyancy inputs from the rivers to the coastal waters and the heat fluxes at the heat fluxes in deeper areas (Frey, 1990; Simpson
40 et al., 1993). It Stratification is also strongly influenced both by the by wind intensity and direction of wind: while the : while westerly winds allow, and the easterly winds enhance stratification, southerly winds have a particularly destratifying effect (Schrum, 1997). An estuarine-like circulation has been shown to be present within the coastal areas of the German Bight (Burchard et al., 2008; Burchard and Badewien, 2015). This mechanism has been suggested to contribute to the maintenance of the steep, cross-shore suspended particulate matter (SPM) and nutrient gradients (Flöser et al., 2011; Hofmeister et al., 2017), with
45 regional differences (van Beusekom et al., 2019). The steep cross-shore gradients observed in SPM and nutrient concentrations have been recently reproduced by numerical models (Staneva et al., 2009; Gräwe et al., 2016) owed to high resolution grids and the terrain-following vertical coordinates that enables enable representation of the estuarine circulation.

Surrounded by industrialized and densely populated countries, the southern North Sea has been experiencing eutrophication related problems (Radach, 1992; Hickel et al., 1993; OSPAR, 2017), such as occasional oxygen depletion events during summer
50 (Frey, 1990; Große et al., 2016). The Elbe and Weser rivers have been estimated to be the primary sources of nitrogen (N) in the southern North Sea (Große et al., 2017). Since the 1980s, nutrient concentrations in these and other contributing rivers (e.g., Rhine, Meuse), have been significantly reduced, more for phosphorus (P) than for N (Radach and Pätsch, 2007), which . This has resulted in some improvement in water quality, especially within the northern Wadden Sea (Wiltshire et al., 2008;
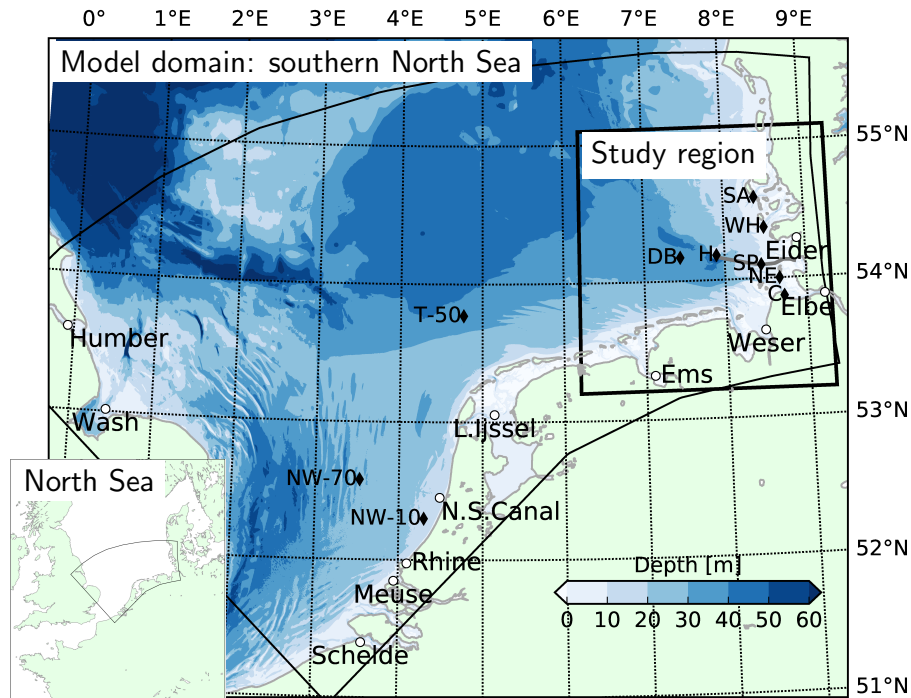
Figure 1. Model domain, bathymetry (data from the European Marine Observation and Data Network, EMODnet), and the location of the study region, the German Bight. Filled circles: location of river mouths on the grid, diamonds: monitoring stations (NW: Noordwijk, T: Terschelling, DB: Deutsche Bucht, H: Helgoland, SP: Suederpiep, SA: Southern Amrum, WH: Westerhever, NE: Norderelbe, C:Cuxhaven), gray line: the average route of the Ferrybox transect between Helgoland and Büsum (see section 2.3).

van Beusekom et al., 2019), but according to a recent study, the nutrient concentrations within the coastal areas are estimated
55 to be still 50-70% higher in comparison to than the pre-industrial state of the 1880s levels (Kerimoglu et al., 2018).

The extent to which the hydrodynamical structure, and the transport of riverine material within the German Bight depends on the inter-annual interannual variability in riverine discharges is not fully understood. In particular, whether and to what extent a flood event would influence the thermohaline stratification within the off-shore waters, or the estuarine circulation at the coastal waters has not been explicitly investigated. In this study, based on the simulations obtained with a coupled physical-
60 biogeochemical model, we examine the physical and biogeochemical structure in the German Bight during July 2013, i.e., following a major flood event (Voynova et al., 2017), in comparison to those in the previous year, July 2012, in order to characterize the sensitivity of the hydrodynamical and biogeochemical structure within the German Bight to the meteorological and hydro-logical conditions. Through a numerical scenario analysis, we try to disentangle the effects of the flood event, meteorology, and in particular the wind conditions.

2 Material & Methods

2.1 The Model

The hydrodynamical host, the General Estuarine Transport Model (GETM, Burchard and Bolding, 2002) is a free-surface baroclinic model that uses terrain-following vertical coordinates. GETM was previously applied to the greater North Sea area (Stips et al., 2004; Pätsch et al., 2017) and the German Bight and Wadden Sea regions in higher resolution (Staneva et al., 2009; Gräwe et al., 2016). In the current application, GETM is defined on a curvilinear grid with a resolution of 1.5-4 km (Fig. 1) and 20 vertical layers, and operated with integration time steps of 5 s and 360 s for the barotropic and baroclinic modes, respectively. At the northern and western boundaries, surface elevations extracted from TRIM-NP-2D (Gaslikova and Weisse, 2013) are provided as clamp boundary conditions at hourly resolution (see below for other boundary conditions). For the discretization of advection, we employed a third order, total variation diminishing P2-PDM (i.e., ULTIMATE QUICKEST) scheme, recognized for its accuracy and gradient conserving qualities (e.g., Pietrzak, 1998; Burchard and Rennau, 2008).

An almost identical model setup was previously employed and shown to capture the spatial and temporal distributions of temperature and salinity within the German Bight for the period 2000-2010 (Kerimoglu et al., 2017a), as well as the tidal dynamics (Nasermoaddeli et al., 2017)(Nasermoaddeli et al., 2018). Since then, the following refinements were made: *i*) providing meteorological forcing at hourly resolution extracted from a COSMO-CLM hindcast simulation (Geyer, 2014), which was previously at 6-hr resolution; and *ii*) specifying the monthly average vertical temperature and salinity profiles at the boundaries for each year separately as predicted by HAMSOM (for a recent description of the setup, see Große et al., 2017), instead of providing climatological averages for all years; *iii*) explicitly describing the horizontal diffusion through a Smagorinsky parameterization (Smagorinsky, 1963). Impacts of the first two refinements *i-ii* were subtle and local, but introduction of the horizontal diffusion horizontal diffusion (*iii*) systematically improved the representation of coastal gradients, and resulted in more plausible total mixing rates overall (see Appendix A).

The biogeochemical model employed here, provisionally named 'Generalized Plankton Model' (GPM), has been recently developed. It has two main components: a component that describes plankton dynamics, and a geochemistry component that describes the recycling of the organic material within the water and sediments. These compartments, both of which are implemented as FABM (Framework for Aquatic Biogeochemical Models, Bruggeman and Bolding (2014)) modules, are coupled in run-time. Elemental fluxes between various model compartments are illustrated in Fig. 2.

The plankton component has been developed based on the carbon (C-) and P- resolving generic plankton model, described by Kerimoglu et al. (2017b) in the context of a lake application. Specifically, the extensions included descriptions of N and silicate (Si) limitation of phytoplankton (diatoms for the latter), and variations of the Chl:C ratio according to Geider et al. (1997). Heterotrophs can now handle and properly recycle prey with constant or variable C:N:P:Si ratios. The 'genericity' of the previous model version (Kerimoglu et al., 2017b) was due to the fact that each plankton species was described as a potential mixotroph with a prescribed autotrophy/heterotrophy ratio. In the new version, explicit phytoplankton and zooplankton modules are used, in order to facilitate future development, where phytoplankton-, zooplankton- and mixotroph- specific functionalities are foreseen to be included in future work. In the present application, plankton comprises of two phytoplankton
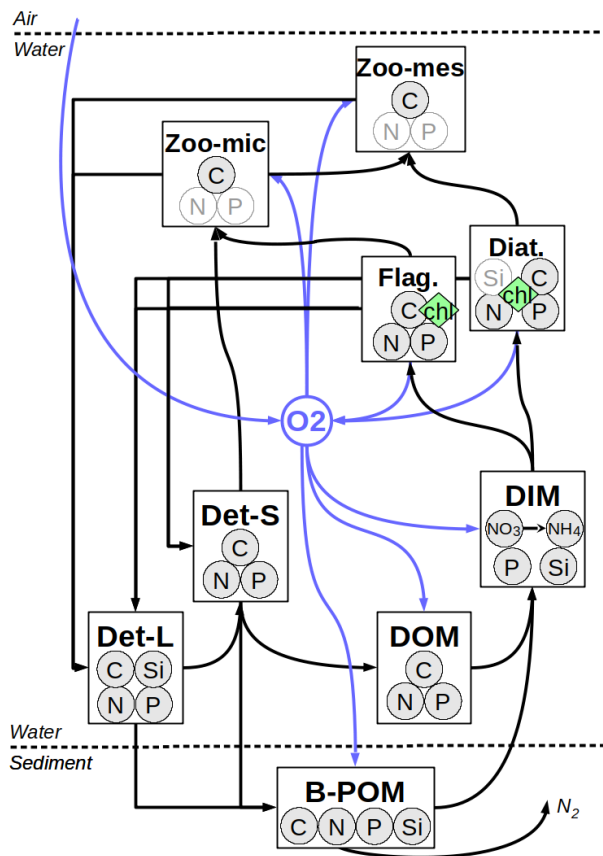
Figure 2. Elemental fluxes between model compartments. Det-L and Det-S: Large large and Small small detritus, DOM: Dissolved Organic Matter, DIM: Dissolved Inorganic Matter, B-POM: Benthic Particulate Organic Matter. The pale N and P in micro- and mesozooplankton and Si in diatoms represent diagnostic state variables which are determined by a fixed prescribed ratio to the C-bound to these pools, resolved as a state variable. For the sake of simplification, fluxes from phytoplankton and zooplankton to DOM and DIM pools are not shown (see Appendix B for a detailed description of model).

functional groups, namely diatoms and nanoflagellatesflagellates, and two zooplankton functional groups, namely , micro- and
100 meso-zooplankton.

The abiotic (geo-chemistry) component is component (i.e., module describing non-planktonic processes) is largely based on ECO-HAM, as described by Lorkowski et al. (2012). This component describes . Description of the dynamics of two detritus size classes, a dissolved organic material (DOM)pool, a pools (large and small), dissolved oxygen, dissolved inorganic material (DIM) pool , a 0-D benthic pool and dissolved oxygen. Light that resolves PO_4, Si, NO_3 and NH_4, and a plate (not vertically resolved) benthic pool are as in Lorkowski et al. (2012).
105 ECOHAM's carbonate cycle was excluded, and a simpler description for DOM remineralization was used. Finally, light conditions are determined by the shading by phytoplankton, detritus, DOM and a parameterization of background turbidity caused by SPM. A detailed description of the model formulations and parameters can be found in Appendix B.

Starting from the initial conditions obtained earlier, the model was spun-up for the period 2008-2010 with the parameterization presented here, as since up to 3 years was found to be necessary for the solutions to converge from arbitrary initial

110   conditions. We then consider considered the period 2011-2014 for the model performance assessment. For the analysis of the years 2012 and 2013, in addition to the reference run, we consider three scenarios in order to investigate the sensitivity of the physical and biogeochemical structure of the system to the meteorological and hydrological forcing: based on the 2013 run (with respect to ocean boundary and initial conditions), the scenario '2013-R12' was ran run with the river forcing of 2012, '2013-M12' was run with the meteorological forcing of 2012. In a third scenario, '2013-W12', only the June-August 2013

115   was simulated with the wind and atmospheric pressure fields from the respective months in 2012, starting from the initial conditions of June 2013 and using the ocean boundary conditions of 2013.

2.2   Riverine and Atmospheric DataForcing

Both for atmospheric forcing of the coupled physical-biogeochemical model, and for the analysis of meteorological conditions, we use an atmospheric hindcastwith the COSMO-CLM atmospheric hindcast, that has a 0.22° resolution (Geyer, 2014). Meteoro-

120   logical forcing from COSMO-CLM comprises precipitation, total cloud cover, mean sea level pressure, relative humidity and air temperature at 2m above sea surface, and U- and V- components of wind at 10m above sea surface, whereas evaporation was calculated by GETM. Shortwave radiation at the surface was calculated according to astronomical functions provided by GETM, and corrected by cloud cover and seasonal variations in surface albedo according to Payne (1972). Longwave radiation was calculated according to Clark et al. (1974). Momentum and heat fluxes were calculated

125   according to bulk formulae by Kondo (1975).

Atmospheric deposition of nitrogen rate of oxidized and reduced nitrogen, added respectively to the modelled NO_3 and NH_4 at the surface layer, was downloaded from the website of the European Monitoring and Evaluation Programme (EMEP)..

Riverine fluxes were maintained and discharges and nutrient fluxes were derived from the OSPAR Comission's ICG-EMO (Intersessional Correspondence Group on Eutrophication Modelling) database, provided by S. van Leeuwen (NIOZ) upon

130   personal request. Variability of discharge rates and concentration of inorganic and organic constituents for the period have been explored by Radach and Pätsch (2007)Here, we considered only the major rivers shown in Fig. 1 (Witham, Welland, Nene and Great Ouse are collectively labeled as the 'Wash'). Based on Amann et al. (2012), 30 % of the organic material (total minus inorganic form for each of the C, N, P and Si) is assumed to be in particulate form (detritus), and the rest to be in dissolved form (DOM). Small (<30d) gaps in riverine data were filled using linear interpolation, and larger gaps were replaced with long-term (2000-2017) climatologies.

135   Riverine inputs were applied over the full depth, given the fact that the outlets of all considered rivers are at shallow sites (Fig. 1).

2.3   Observation data

Station data (Helgoland, Cuxhaven, Deutsche Bucht(German Bight), ; see Fig. 1for the locations) for temperature, salinity and oxygen (the latter only at Deutsche Bucht) were downloaded from the COSYNA (Coastal Observing System for Northern and Arctic

140   Seas) data portal (www.cosyna.de, see Breitbach et al., 2016) at daily resolution (snapshots at 00:00 averaged within a 3600 s an

hourly time window). Collection and processing of the semi-continuous data collected by FerryBox platforms at the Cuxhaven and Helgoland monitoring stations and on the M/V *Funny Girl* ferry operating between Büsum and Helgoland during May-September have been described previously by Petersen et al. (2011) and Voynova et al. (2017) and are available from the COSYNA data portal as well.

145   N, P, Si and chlorophyll data at the Helgoland-Roads station was were collected at semi-daily (every working day), and using standard procedures as described by Wiltshire et al. (2008). Data from the Noordwijk, Terschelling, Norderelbe, Suederpiep and Westerhever stations are available at monthly intervals. For the Noordwijk-70 and Terschelling-50 stations, we consider only the surface measurements available at biweekly intervals, while the data at other stations are located at shallow sites, and therefore provide only surface measurements. Mooring data for surface (<10 m) salinity, temperature and nutrients, randomly

150 distributed over the entire model domain and simulation period 2011-2014, were obtained from the International Council for the Exploration of the Sea (ICES). In this dataset, the outliers, defined as the values falling outside the $[\bar{o} \pm 4\sigma]$ range, where $\bar{o}$ and σ stand for the mean and standard deviation of the raw observations, were removed.

     Spatial matching of all data was performed by calculating the distance-weighted mean of the nearest four modelled grid values around the observation, using the 'spatial.cKDTree' package from the Scipy library, version 1.1.0 of Python 3.5.

155 ## 3   Results

3.1   Hydrological and Meteorological Conditions

Variability of discharge rates and concentration of inorganic and organic constituents for the period 1977-2000 was explored by Radach and Pätsch (2007). Here, we analyze the discharge and nutrient fluxes for the specific time period of interest. Typically, the discharge rates of the continental rivers around the southern North Sea peaks peak during winter/early

160 spring (e.g., Lenhart et al., 1997). Flow rates of For the rivers Elbe, Weser and Ems during , the major rivers discharging to the German Bight, this pattern holds for the decade that includes and precedes the time period of interest, and 2012 and 2013 follow this typical pattern in particular (Fig.3) but . But during June 2013, a large precipitation event over the central Europe caused flooding of all several major river basins in Germany (Merz et al., 2014), including Elbe and Weser (Fig.3). The Elbe flood ocan can be considered as a 100-year event with discharge rates of up to 4060 m^3 s^{-1} during 11 and 12 June (Voynova et al., 2017),

165 which is four-fold higher than the typical discharge rates during winter (Fig.3). Ems, and the other rivers in the model domain do not show such an extreme response, underlining the locality of the aforementioned meteorological event. Nitrogen, phosphorus and silicate concentrations did not vary systematically during the flood event, and therefore their fluxes paralleled the discharge rates, with distinct peaks during June 2013 for the Elbe and Weser rivers (Fig.3).

     Meteorological conditions during 2012 and 2013 differed systematically during two periods (Fig. 4). The first of these

170 occurred during the early spring: March 2012 was characterized by relatively warm air temperatures and winds mildly blowing from the west/southwest, whereas March 2013 was cold with strong easterly winds. The second period occurred during the middle of summer: July 2012 was relatively cold with overcast skies and some precipitation, contrasting with warmer, drier and calmer conditions in July 2013.
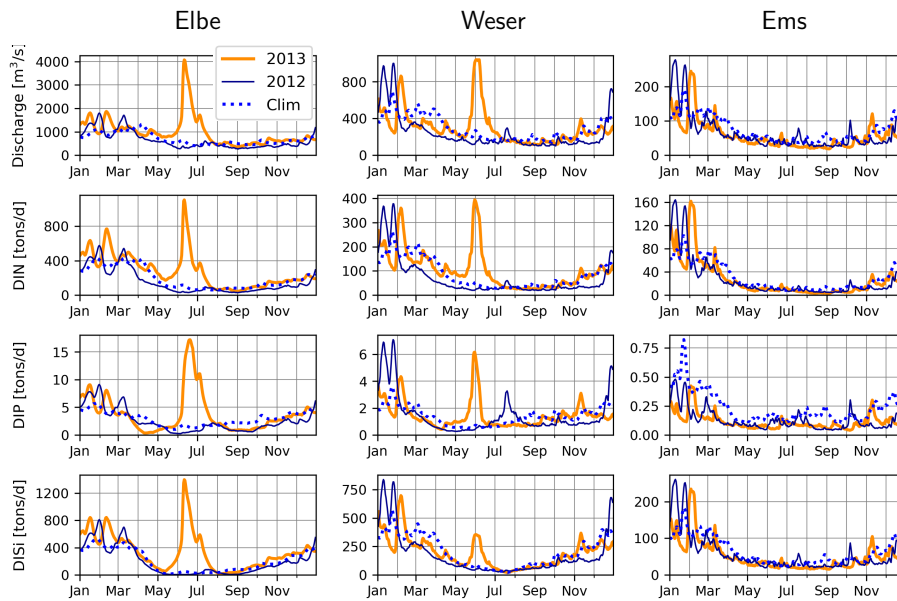
Figure 3. Measured discharge, DIN (NO3+NH4 NO_3+NH_4), DIP and DISi loading rates at rivers Elbe, Weser, and Ems during 2012 (dashed dark blue lines) and, 2013 (red orange lines) and the 2005-2014 climatology, excluding 2013 (dashed blue lines).

3.2 Assessment of the Model Performance

175 Simulated temperature and salinities at the surface match well to , in general, well the observations found in the ICES database, randomly distributed throughout the model domain within the period 2011-2014 (Fig. 5), and exhibit no signs of systematic deviations or biases. There is a slight cold bias at the lower temperature range (29-32 g/kg), which seems to be canceled out by the slight warm bias at the higher range. These deviations are mostly within a 1 °C range, therefore presumably do not have a significant effect. At an intermediate range, salinity is overestimated by up to 2 g/kg, indicating insufficient spread of

180 coastal waters with low salinity. This may either be due to (still) underestimated horizontal mixing (see Appendix A), or inaccuracies in the advection patterns. Match of the simulated NO3 NO_3 and DIP to the ICES-observation set is reasonably well, with -5% normalized bias and correlation coefficients larger than 0.6 for both variables (Fig. 5). Underestimated NO_3 at an intermediate range (10-40 μMN) is possibly due to the aforementioned underrepresentation of N-rich riverine waters within the transition zone. Regarding DIP, the measured-simulated pairs that represent major underestimation errors

185 (e.g., in the <0.5 μMP simulation band) point to the inability of the model to capture summer maxima occurring in specific coastal regions.

Comparison of simulated Simulated and measured temperature and salinity are compared at 3 fixed monitoring stations are shown in (Fig. 6). Two of these stations, Helgoland and Cuxhaven are located at shallow sites, therefore provide only surface measurements, whereas the third one, the Deutsche Bucht, provides measurements also at 30m depth. At all these stations, temperature

190 is estimated with 5-9% negative bias, and correlation scores ranging range between 0.99-1.0. The inter-annual interannual variations
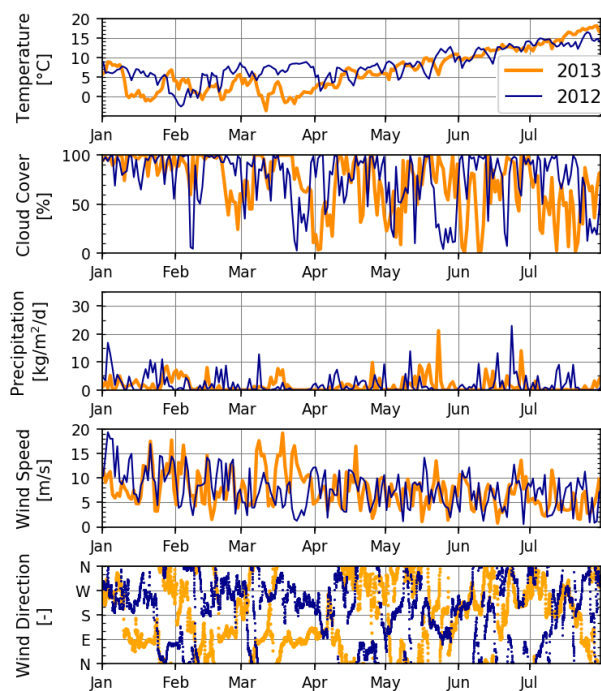
Figure 4. Meteorological variables during January-July 2012 and 2013, extracted from a representative grid point (54°14'N, 7°29'E) of the meteorological hindcast, used also as model forcing (see Section 2.2). Temperature is from 2 m and wind is from 10 m height above the sea level. Wind direction is shown at hourly resolution, all other variables at daily resolution.

are well captured: the relatively warm winters (January-March) of 2012 and 2014, and the cold winter of 2013 manifest as cold and warm water temperatures according to the observations, and these differences are realistically reproduced by the model, despite the modeled temperatures being about 0.5 to 1.0 K -1.0 °C lower. Salinity is modelled consistently with only up to 2% bias at all 3 stations, despite the relatively lower correlation coefficients in comparison to temperature (Fig.6). The relatively higher

195 variability of the salinity measurements are is due to the tidal variations (most obvious at the Cuxhaven station), which are smeared out in the daily average model output. The freshwater plume of the flood event of June 2013, and other similar events have been accurately reproduced by the model.

According to the June-July average salinities measured by FerryBox on the M/V *Funny Girl* ferry on its transect between Büsum and Helgoland (Fig. 1), the salinities gradually decrease from about 32 g/kg at Helgoland to about 27 g/kg at Büsum in 2012

200 (Fig. 7). In 2013, driven by the freshwater plume of the flood, the average salinities were lower at both edges, with about 27-29 g/kg at Helgoland and 22-23 g/kg at Büsum. The model estimates are quite accurate at the off-shore areas, but undershoot underestimate the observations near the coast, up to 2 g/kg in 2012 and 3-5 g/kg in 2013. Despite these biases, the clear difference between the two years as captured by the FerryBox is qualitatively captured by the model.

9
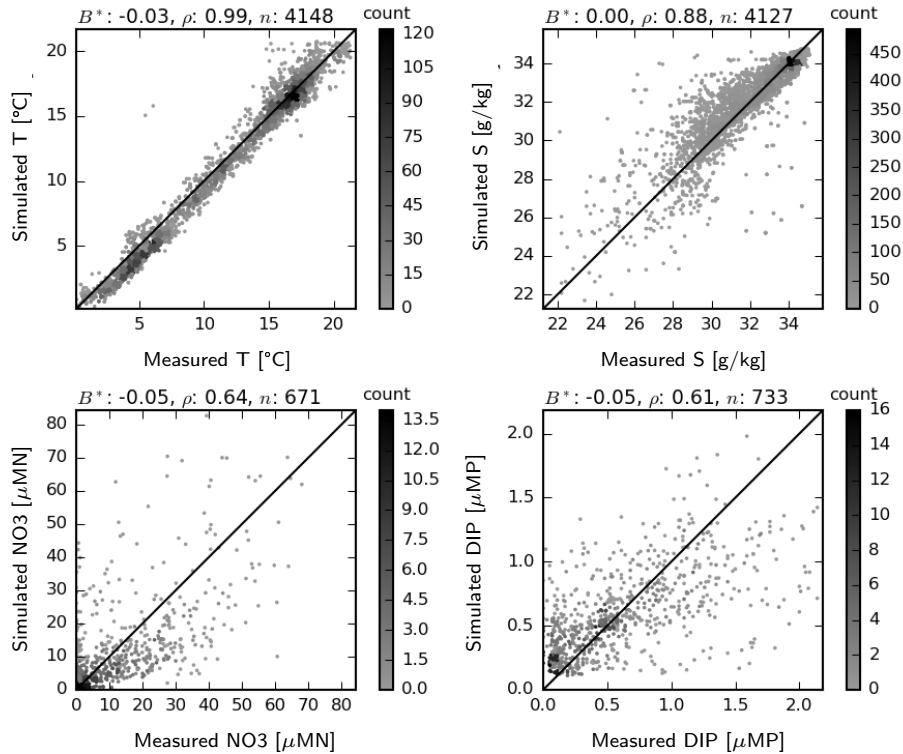
Figure 5. Simulated Two dimensional histogram of simulated vs measured temperature, salinity, NO3 NO$_3$ and DIP at the surface for the period 2011-2014. Count indicates the occurrence frequency of simulation-observation pairs. $B*$: normalized bias, ρ: correlation coefficient, n: number of observation-simulation pairs.

Dissolved inorganic N (DIN, which in our model comprise NO3 and NH4, as NO2 NO$_3$ and NH$_4$, as NO$_2$ was not considered)
205 and P (DIP, i.e., PO4) are generally well reproduced at all monitoring stations considered considered monitoring stations (Fig.8), as suggested by low bias and moderate correlations. The ability of the model to capture the sharp increase in DIN during June/July 2013 at the Helgoland station suggests that the spreading of the plume of the Elbe-Weser rivers following the flood event was realistically reproduced. For dissolved silicate, DISiSi, model estimates overshoot the observations by about 50% at Helgoland and up to 100% at the Noordwijk stations. Latter The latter is mainly driven by the strong DISI DISi fluxes from the western boundary, reflecting the overestimation of Si specified at the
210 boundaries (Fig. 1).

For chlorophyll, there is up to 120% positive bias at the off-shore stations (Fig.8), while the correlation coefficients are particularly low at the Terschelling-50 and Noordwijk-70 stations and moderate at Helgoland and Noordwijk-10. A consistent source of error seems to be the failure of the model to estimate the timing of the spring bloom. However, differences between stations, i.e., values at Helgoland and Noordwijk-10 being higher than at Terschelling-50 and Noordwijk-70 stations, are well
215 reproduced.

10
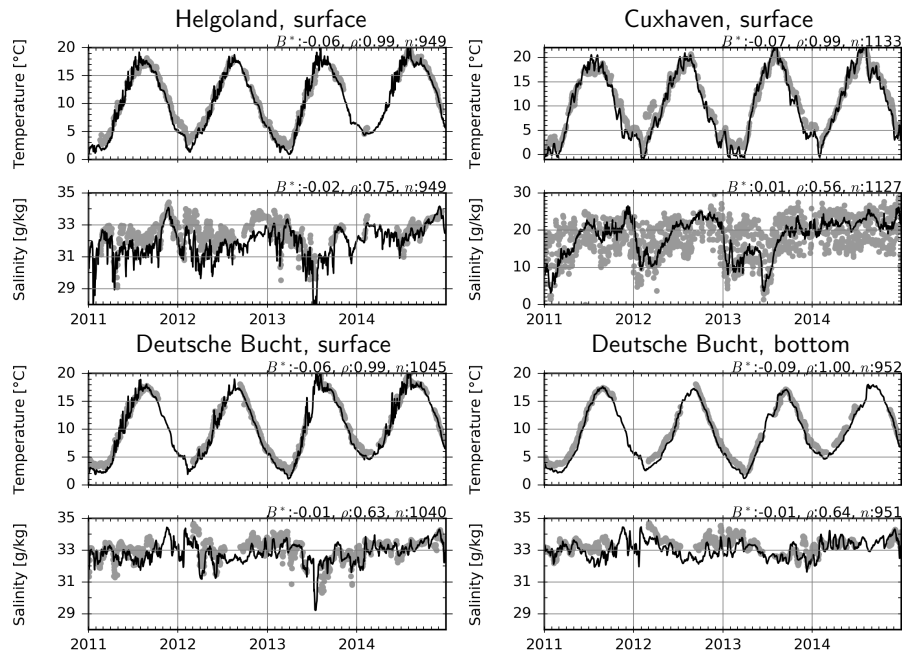
Figure 6. Observations (dots) and model estimates (lines) of temperature and salinity. $B*$: normalized bias, ρ: correlation coefficient, n: number of observation-simulation pairs.
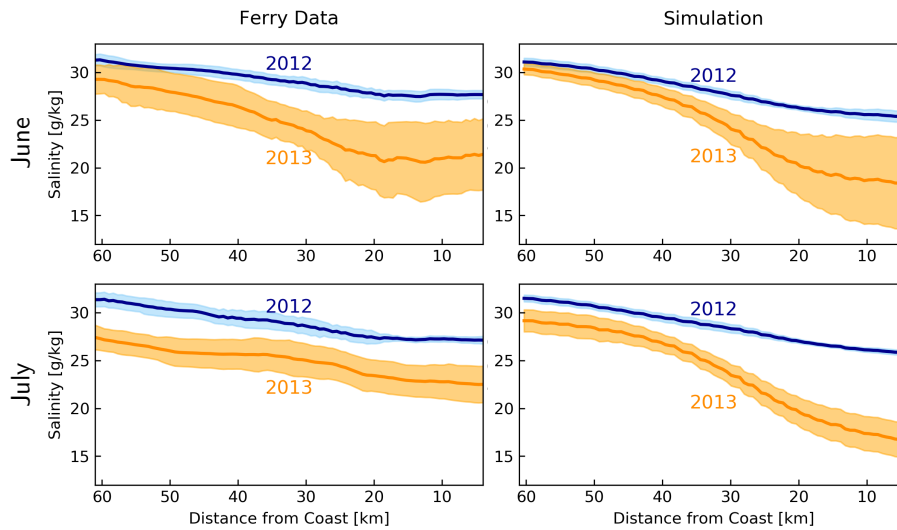
Figure 7. Average (dark lines) and standard deviation (shadings) of salinities between Helgoland and Büsum, according to the FerryBox data from M/V *Funny Girl* and simulation by the model during June and July 2012 and 2013.
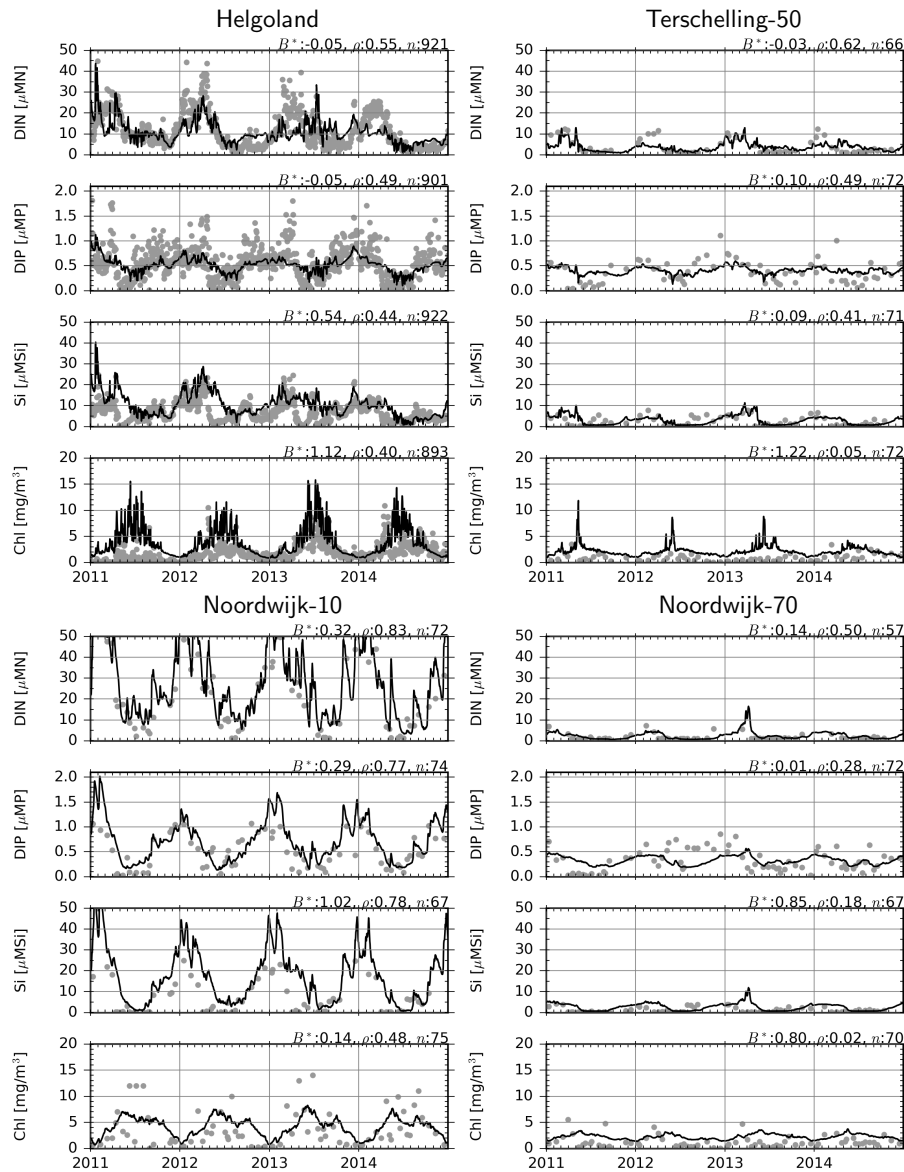
Figure 8. Observations (dots) and model estimates (lines) of surface DIN, DIP, DISi and chlorophyll concentrations. $B*$: normalized bias, ρ: correlation coefficient, n: number of observation-simulation pairs.

Measured and simulated NO3 NO_3 and DIP concentrations at 3 coastal stations, Norderelbe, Suederpiep and Westerhever, located along the North-Frisian Wadden Sea (Fig. 1), are shown in Fig. 9. For the NO3 NO_3, measurements in both June and July 2013 were distinctly higher than those in 2012 at Norderelbe and Suederpiep stations, but not at Westerhever in July. Despite a tendency to overshoot, overestimate, the range of simulated values mostly enclose encloses the measurements, and the

220 qualitative differences between 2012 and 2013 and ~~among~~ **between** different stations were captured by the model. Average DIP measurements did not differ between 2012 and 2013, but gradually decreased with distance ~~to~~ **from** the Elbe mouth. The model captures this gradual decline~~with distance~~, but the difference it suggests between the two years at the Norderelbe and Suederpiep ~~station~~ **stations** in July is larger than **that indicated by** the measurements.
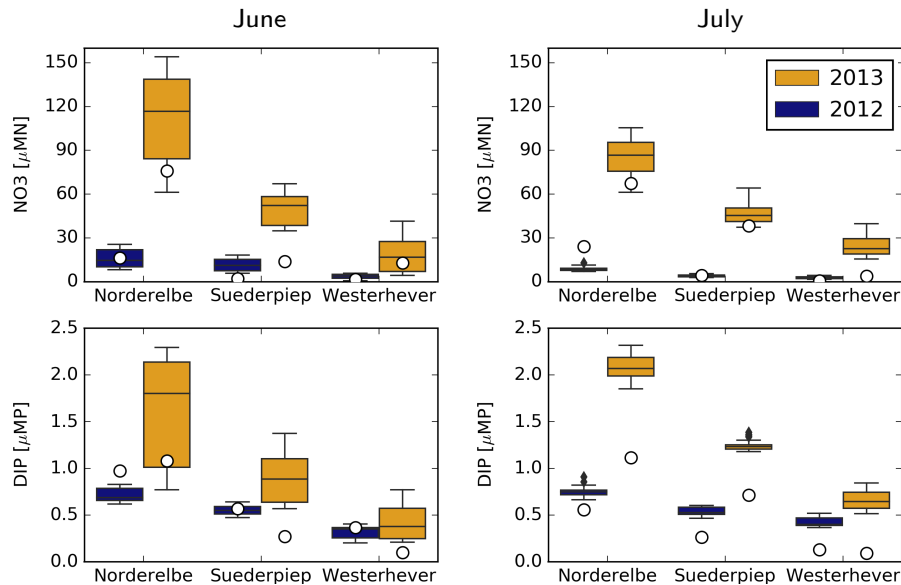
Figure 9. Monthly average measurements (circles) and temporal distribution of the simulations (boxes showing the median, 1st and 3rd quartile and whiskers showing the minimum and maximum values) for surface ~~NO3~~ **NO$_3$** and DIP concentrations at three coastal stations shown in Fig. 1.

3.3 Thermohaline structure, nutrient status and productivity of the system

225 Average salinities in the surface and bottom layers estimated by the model suggest considerable extension of the Elbe-Weser ROFI during July 2013, in comparison to July 2012 (Fig. 10). This extension is similar in surface and bottom layers within the well mixed shallow areas, but stronger at the surface in deeper regions where a thermohaline stratification develops (Fig. 11). The surface and bottom temperatures display similar horizontal gradients during July 2012 and 2013 with higher temperatures near the coast, and lower temperatures within the offshore regions (Fig. 10). However, the surface temperatures within the outer

230 areas during July 2013 are 1-2 ~~K~~ **℃** higher than those during July 2012 (Fig. 4). In contrast, the bottom temperatures during 2013 July are lower than those during July 2012.

When the riverine forcing of 2012 was used for simulating 2013 ('2013-R12' scenario), the characteristic freshwater plume of 2013 disappears (Fig. 10). The resulting freshwater front (e.g., as hinted by 30 g/kg isohaline) differs from that ~~in~~ **of** 2012 as well, having retreated to the southern latitudes. Under this scenario, the temperatures at the bottom layers remain identical to those of 2013, but the surface layer becomes slightly colder. The latter is explained by the increasing stability of the water

13
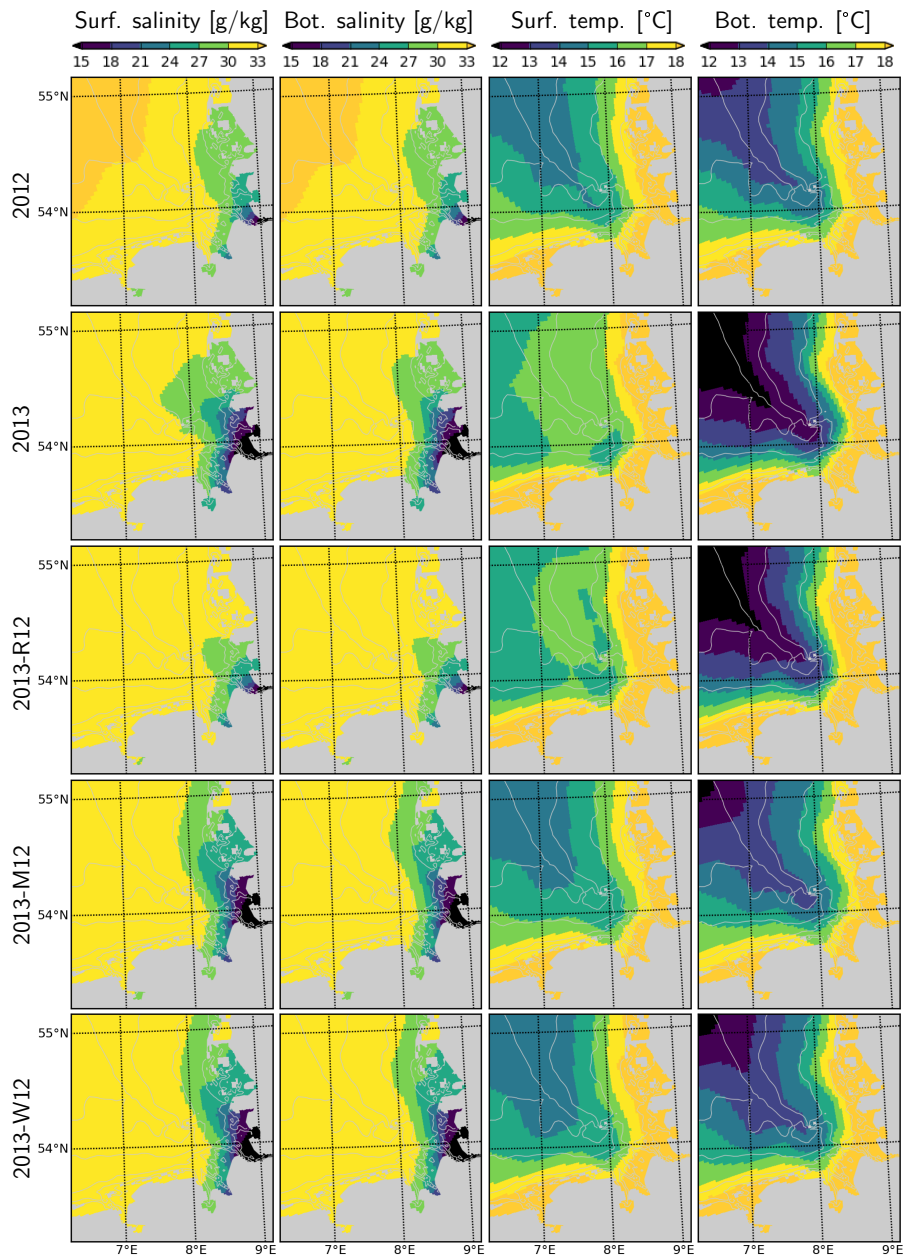
Figure 10. Salinity and temperature in the surface and bottom layers during July for the years 2012 and 2013 and scenarios 2013-R12, 2013-M12 and 2013-W12.

column due to the extra buoyancy caused by the flood event in 2013, reflected by the larger area of intense (>1 kg m^{-3}) density stratification (Fig. 11, compare 2013 and 2013-R12).
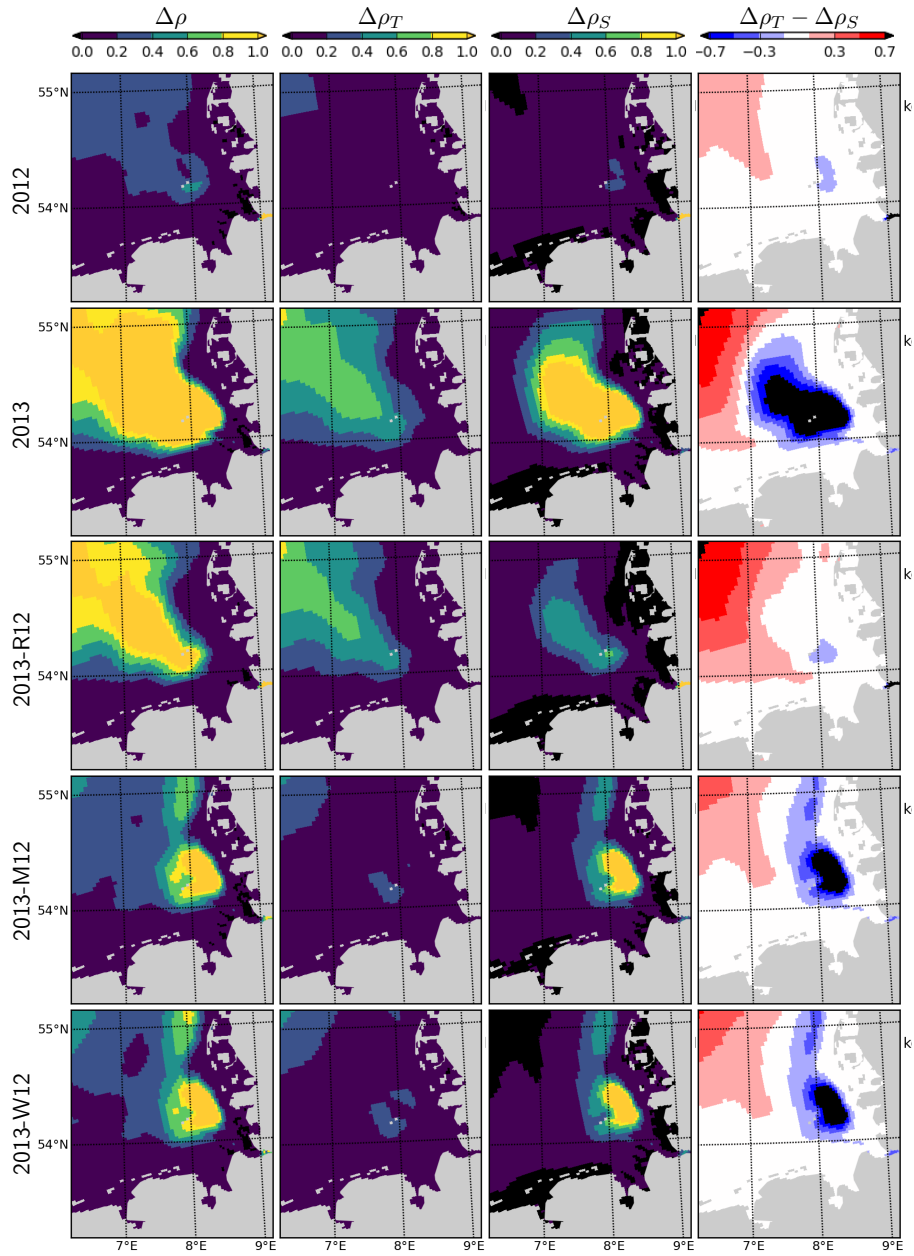
Figure 11. Density difference between the surface and bottom layers ($\Delta\rho$), contribution of temperature and salinity, ($\Delta\rho_T$ and $\Delta\rho_S$ as estimated by the linearized equation of state: $\rho - \rho_0 = \alpha(T - T_0) + \beta(S - S_0) + \gamma(P - P_0)$, with α = -0.15 kg m^{-3}/K and β = 0.78 kg m^{-3} / (g kg $^{-1}$) see the text), and their difference ($\Delta\rho_T$ - $\Delta\rho_S$), during July for the years 2012 and 2013 and scenarios 2013-R12, 2013-M12 and 2013-W12.

Effect The effect of exchanging the entire meteorological conditions forcing (as indicated by the 2013-M12 scenario), and only that of compared to that of exchanging only the short-term (i.e., starting from June) wind forcing (2013-W12 scenario) on the

240 salinity distribution is almost identical: according to both scenarios, the freshwater plume around the mouth of Elbe and Weser is preserved, but the plume spreads along the coast instead of spreading towards the outer German Bight as was the case in the original 2013 simulation (Fig. 10). Thus, it can be concluded that the distribution of salinity within the central and outer German Bight in July 2013 can concluded to be is driven by the short-term wind conditions. The freshwater front (e.g., as indicated by the 27-30 g/kg isohalines), simulated according to both 2013-M12 and 2013-W12 scenarios extend further to , extends further

245 to the North in comparison to 2012, which is evidently driven by the additional freshwater inputs due to the flood.

Temperatures simulated according to 2013-M12 scenario are similar to those simulated for 2012, characterized by relatively low temperatures at the surface and the relatively high temperatures at the bottom, in comparison to the original estimations for 2013. Interestingly, the temperatures simulated by the 2013-W12 scenario are similar to those simulated by the 2013-M12 scenario, indicating that the large differences in surface and bottom temperatures during July 2013 was were mainly caused by

250 the wind conditions. In the 2013-W12 scenario, enhanced turbulent vertical mixing, driven by the stronger winds of the in July 2012 does not allow the surface temperatures to build up, while it causes the cold bottom temperatures to increase to the levels originally simulated for July 2012, except within the northeastern northwestern margin of the study region, where the bottom temperatures remain cold.

The combination of temperature and salinity dynamics determines the 3-dimensional density (ρ) structure of the system.

255 The difference between the density of the surface and bottom layers ($\Delta\rho$) therefore indicates the intensity of the thermohaline stratification, and hence, gives insight into the average light conditions primary producers experience in the deeper zones surface layers. Average $\Delta\rho$ during July 2012 indicate a weak stratification in the outer German Bight with values mostly below 0.4 kg m^{-3}, with the exception of a small patch south of Helgoland (Fig. 11). During July 2013, $\Delta\rho$ displays an area of strong stratification ($\Delta\rho > 1.0$ kg m^{-3}) penetrating to the inner German Bight along the old Elbe Valley. Contributions of

260 temperature and salinity to the $\Delta\rho$, i.e., $\Delta\rho_T$ and $\Delta\rho_S$, as approximately estimated by the linearized equation of state ($\rho - \rho_0 = \alpha(T - T_0) + \beta(S - S_0) + \gamma(P - P_0)$, with α = -0.15 kg m^{-3}/K and β = 0.78 kg m^{-3} / (g kg $^{-1}$)) suggests that $\Delta\rho_S$ is larger than $\Delta\rho_T$ in a region surrounding and extending northwest of Helgoland. The 2013-R12 scenario results in a $\Delta\rho$ similar in intensity and shape to that in 2013, only narrower in the inner German Bight, whereas the $\Delta\rho$ estimated by the 2013-M12 and 2013-W12 scenarios are small within the outer areas as in 2012, but forms a strong large patch located northeast

265 of Helgoland.

Simulated DISi and DIN plumes of Elbe in 2013 July following the flood event (Fig. 12) resemble the freshwater plumes (Fig. 10). This plume disappears when the river forcing of the 2012 is used (2013-R12) and it gets pushed along the eastern coast in the 2013-M12 scenario (Fig. 12), similar to the freshwater plume (Fig. 10). The plume of the DIP on the other hand, when scaled to the Redfield proportions (molar N:P=16), is confined to a smaller region closer to the Elbe estuary. Thus, the

270 impact of the river plume on the nutrients can be tracked by the enhanced N:P ratios.

Spatial distribution of the water-column integrated net primary production rate, NPPR is considerably different in July 2013 than in July 2012 (Fig. 12). Two areas with prominent changes can be distinguished: *i)* outer German Bight (OGB), i.e., west of 7.5 °E and north of 54.5 °N; *ii)* central German Bight (CGB), i.e., region around Helgoland, and its westward and northward extensions. Within the OGB, NPPR estimated for 2013 is lower than 2012 and by 2013-M12/W12. This can
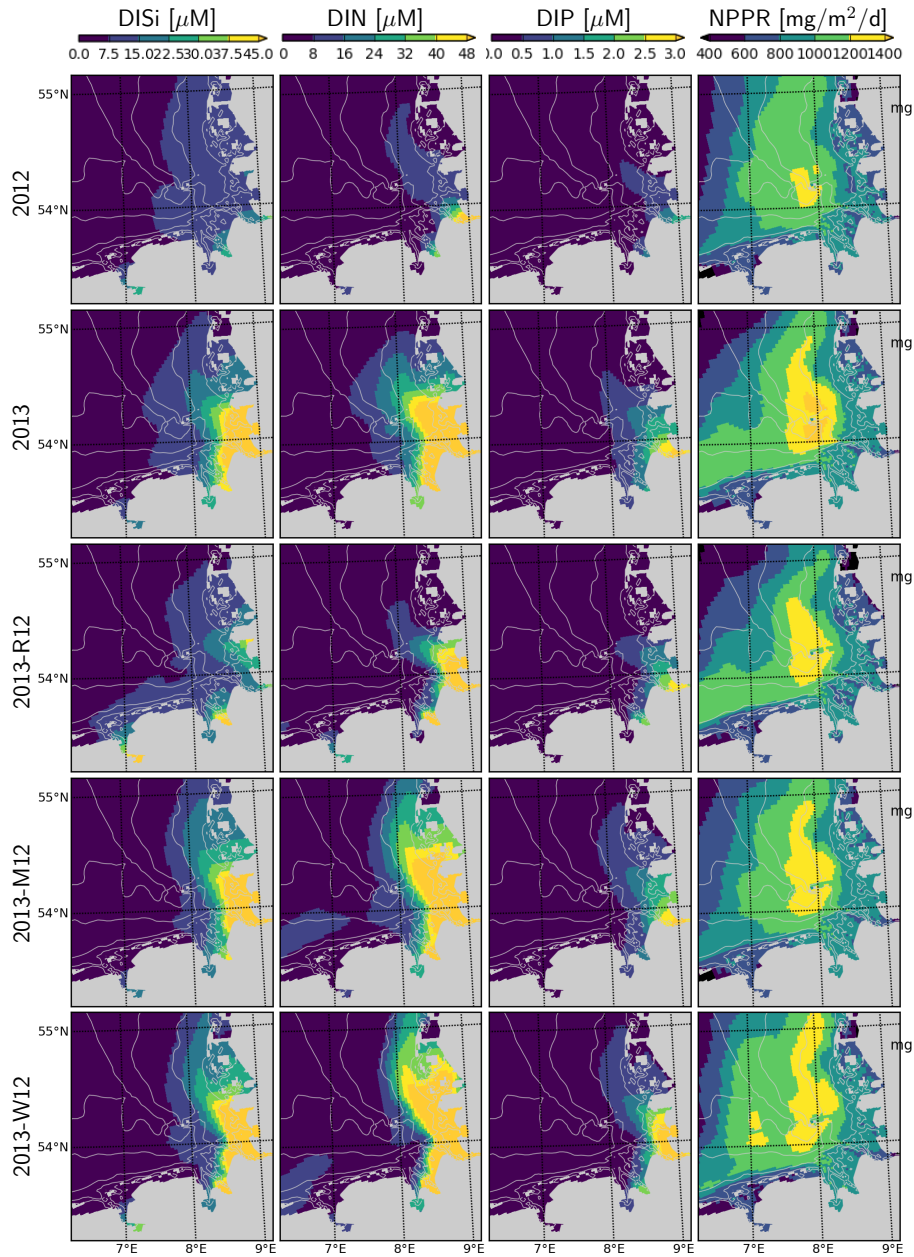
Figure 12. Surface DISi, DIN, DIP and integrated net primary production rate during July for the years 2012 and 2013 and scenarios 2013-R12, 2013-M12 and 2013-W12.

be explained by the nutrient limited phytoplankton growth in this region, and the intensification of nutrient limitation due to stronger stratification in 2013 driven by meteorological conditions (Fig. 11). Within the CGB, the distinctive patch of high NPPR that is narrowly present in July 2012 expands considerably in July 2013. In comparison to 2013, the 2013-R12 scenario

results in a weakening of NPPR within the entire CGB, in terms of both peak rates and areal coverage of high values, especially in the northern portion. The 2013-M12/W12 scenarios also lead to local reductions of the peak rates achieved at around and north of Helgoland, pointing to the relevance of the hydrological conditions for the intensity of NPPR during July 2013. The enhancement of NPPR within the CGB can be explained by the enhancement of light conditions due to strong stratification in this nutrient-rich region, especially following the flood event (Fig. 12).
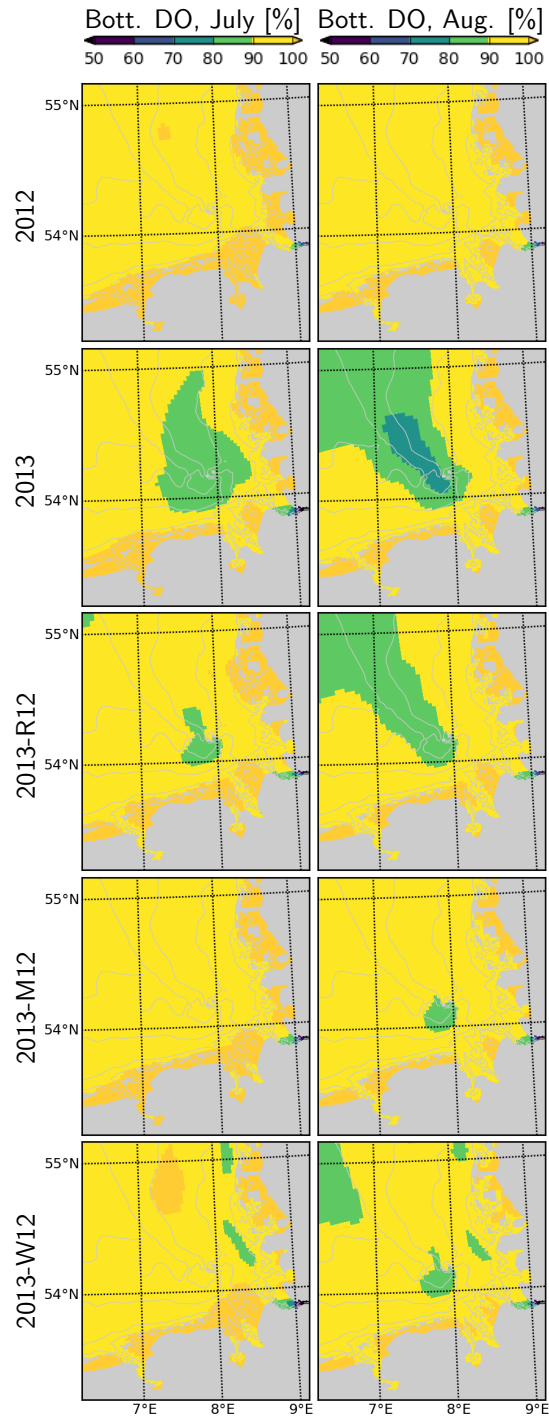
Figure 13. Dissolved oxygen in bottom layers during July and August, for the years 2012 and 2013 and scenarios 2013-R12, 2013-M12 and 2013-W12.

In 2012, the Dissolved Oxygen (DO) remains close to saturation (Fig. 13). In contrast, in July 2013, a widespread patch of oxygen undersaturation (< 90% of saturation) develops within the bottom layers of the CGB. This further intensifies (< 80%) and expands towards the OGB during August 2013. Occurrence of this oxygen undersaturation can be explained by the enhanced DO consumption, fueled by the increased NPPR within the CGB (Fig. 12) and the intense stratification within the entire German Bight (Fig. 11) that limits the oxygenation of the bottom layers. In the OGB, the widespread oxygen undersaturation despite the lower NPPR (Fig. 12), highlights the importance of stratification (Fig. 11). Under the 2013-R12 scenario, oxygen levels do not drop as much as in the 2013 scenario within the CGB, and the area with oxygen undersaturation shrinks especially during July, but also in August. The 2013-M12 and 2013-W12 scenarios result in a complete disappearance of the oxygen undersaturation within the CGB during July, pointing to the effectiveness of wind-induced mixing in the oxygenation of bottom layers. Within the OGB, oxygen falls below sub-saturation levels in August according to the 2013-W12 scenario, that can be explained by the thermal stratification obtained in this region with this scenario (Fig. 11).
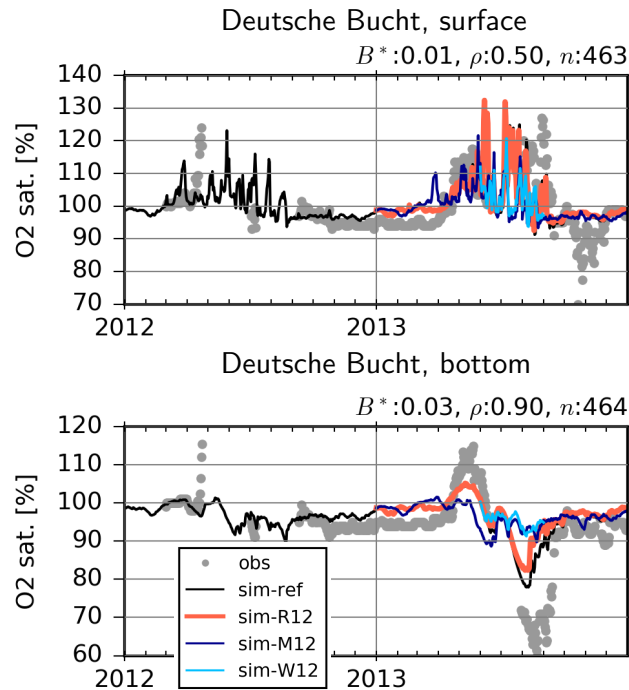
Figure 14. Oberved (dots) and simulated (lines) dissolved oxygen in the surface and bottom layer at the Deutsche Bucht station. $B*$: normalized bias, ρ: correlation coefficient, n: number of observation-simulation pairs based on the reference (ref) run.

At the Deutsche Bucht station, where the temperature and salinity measurements were shown to be reasonably reproduced (Fig. 6), the DO measurements are also mostly well reproduced (Fig. 14). Importantly, the higher levels of supersaturation during 2013 in comparison to 2012, driven by higher NPPR (Fig. 12), and the oxygen depletion in the bottom layers in 2013, and the lack thereof in 2012 are qualitatively captured, although the DO depletion in 2013 is not fully reproduced. Especially

the 2013-M12/W12, and to a lesser extent, 2013-R12 scenarios result in lower levels of supersaturation at the surface, indicating lower levels of NPPR (Fig. 12). At the bottom, especially the 2013-M12/W12 scenarios result in the disappearance of the oxygen drawdown in July 2013, which is driven by both lesser amounts of organic material to degrade as a result of lower NPPR, and the oxygenation of bottom layers via vertical mixing caused by the windy conditions of 2012. The 2013-R12 results in a lower level of drawdown in comparison to the reference (2013) simulation, and an earlier recovery back to the saturation levels.

In order to demonstrate the effects of the thermohaline structure on the current velocities, we consider two specific days characterized by different wind regimes in June 2013, and compare the original estimates with those obtained with 2013-R12 scenario (Fig.15). In order to remove the movements caused by lunar (M2) tides, the current velocities with 30 min. resolution were averaged over 25h intervals, centered around 12:00 of each day. Differences between the two simulations (Fig.15b,e) reveal an increase in current velocities at the surface within the zone affected by the river plume. In the bottom layers, differences occur as well, but these are smaller in magnitude (not shown).
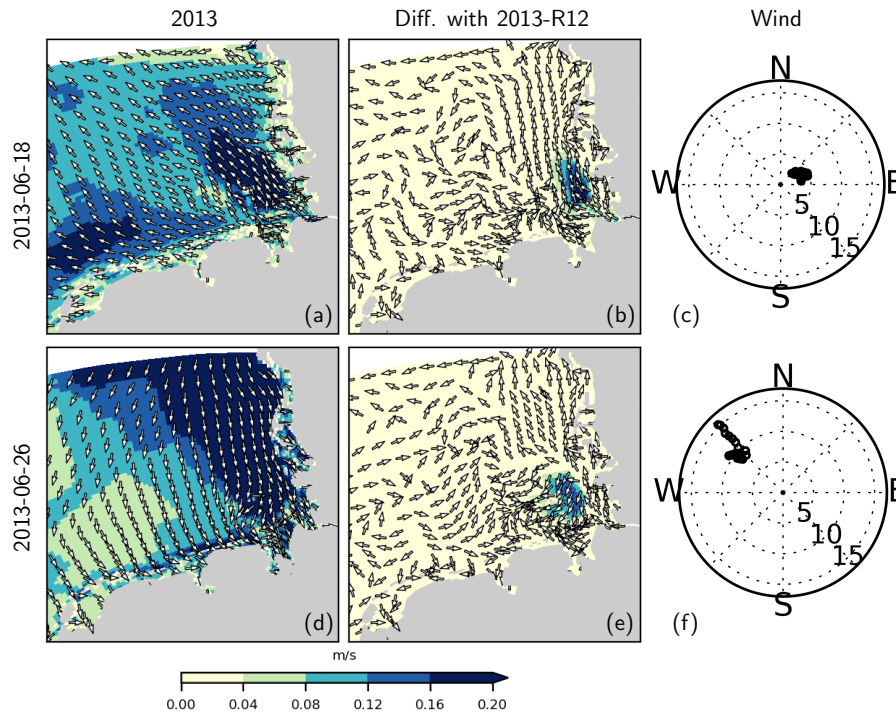
Figure 15. 25h-averaged (residual) current velocities at the surface (a,d) and the difference with those obtained with 2013-R12 , during two different wind conditions (c,f). In panels c,f, wind speed at each hour within the day is marked, with distance from origin indicating wind speed, in m/s.

For a better understanding of the modulation of the flow structure by the flood event within the coastal zone, we elaborate 3 cross-shore transects, two of which cross through the monitoring stations, nutrient concentrations at which were displayed in

Fig. 9), and for . We focus on the conditions during 18 June 2013 that was considered in Fig. 15e-h, regarding the surface current velocitiesa-c, characterized by low wind speeds. On this particular day, an estuarine-like circulation is strongly manifested along the
315 southern part of the north-Frisian Wadden Sea (see Fig. 1), with the cross-shore (x-) velocities at the bottom layers directed towards the shore, and at the surface directed off the shore (Fig.16). Removal of the flood event, as predicted by the 2013-R12, results in a weakening of the bottom currents at the southern section (as represented by Suederpiep) and the middle section (as represented by Westerhever). The along-shore (y-) velocities at in the bottom layers, directed towards south (outwards the plane) display a similar weakening of the bottom currents. These results indicate that provide evidence for the determination of
320 the efficiency of estuarine circulation is determined by an interplay between the meteorological and hydrological conditions, which are subject to spatio-temporal variations.
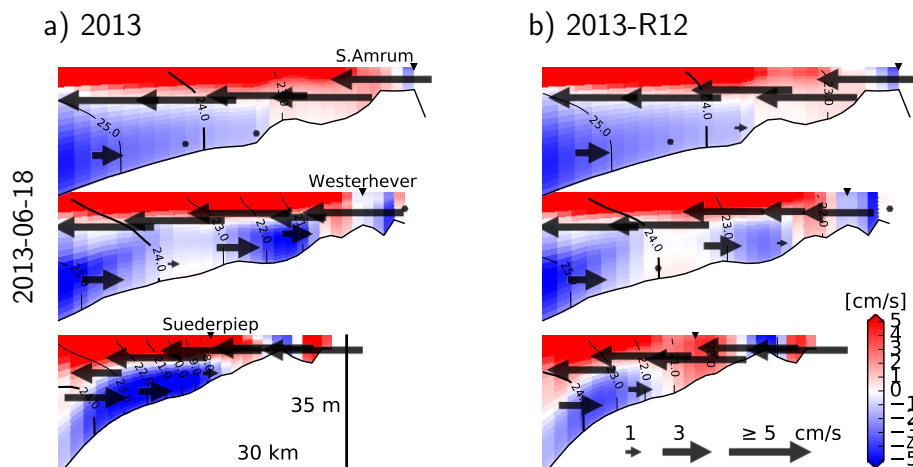
Figure 16. 25h-averaged velocity and density structure simulated with the reference model (a) and with the riverine forcing of 2012 (b), under the northeasterly winds on June 18, 2013 (see Fig.15). Two of the transects cross from the stations shown in Fig.9 (marked by ▼ symbols). Arrows indicate the cross-shore velocities, and the colors indicate along-shore velocities with positive values indicating northward flows (i.e., inward the drawing plane). Contour lines indicate σ_T.

4 Discussion

4.1 Model Performance

In comparison to the performance of the previous version of the hydrodynamical model setup presented by Kerimoglu et al.
325 (2017a), the ability of the model in representing the cross-shore salinity gradients has been significantly improved, mainly due to the introduction of flow-dependent horizontal diffusion (e.g., Fig.A1). As suggested by the comparisons with ICES data (Fig. 5), realism of temperature has also been improved, with the normalized bias decreasing from -0.11 to -0.03, and the correlation increasing from 0.95 to 0.99 (compare with Fig. 4 of Kerimoglu et al. (2017a)). There have been incremental improvements

in the prediction of nutrient concentrations as well. However, these minor deviations may be related with to the differences in specific time periods of interest (2006-2010 in the former study vs 2011-2014 in this study).

The underestimation of salinities (Fig. 7), and consequently the overestimation of nutrient concentrations along the coast (Fig.9) are possibly related with the underestimated due to underestimating the flushing rate at the coastal zone. The insufficient spread of coastal waters is potentially the reason for overestimated salinities and underestimated NO_3 in the transition zone, characterized by intermediate salinities and NO_3 concentrations (Fig. 5). These errors, in turn, may have lead to an over- and underestimation of the importance of riverine discharges on the stratification dynamics and productivity in the coastal and transition zones, respectively. Before the application of explicit horizontal diffusion, these errors were much larger (Appendix A). Application of higher horizontal diffusion rates (e.g., via higher Smagorinsky coefficient C_S, see Appendix A) further improved the model performance along the east Frisian Wadden Sea, however, . However, this was at the cost of overestimation of salinities at the mouth of the estuary, such as at the Cuxhaven station (Fig.6); , as well as further dampening of the tidal amplitudes, which are were already slightly underestimated (not shown). A spatially variable C_S field, with gradually decreasing values at the mouth of the Elbe helped circumventing this problem, but this spatially variable parameterization was not adopted in this study. Before resorting to such ad-hoc solutions, other potential sources of error needs need to be assessed.

A potential source of bias in salinity and nutrients along the Elbe-plume is the misrepresentation of the Elbe estuary in our model setup (Fig. 1). For instance, according to a recent, high resolution model of the Elbe estuary, the freshwater-saline water transition (0-5 g/kg) occurs at about 50-75 km upstream of the mouth of Elbe (under normal hydrological conditions), and the N and Si concentrations vary considerably within the estuary (Pein et al., 2019). Indeed, a high resolution (300m)setup of the German Bight that resolves up to 150 km upstream the Elbe mouth (Chegini et al., submitted) demonstrated better skill in reproducing the salinity observations shown in Fig.7 and Fig. A1. Another contingent error source is potential inaccuracies in advective transport rates, e.g., as a result of imperfections in meteorological forcing (Geyer, 2014) or ignoring the effects of off-shore wind-farms on the thermohaline circulation (Carpenter et al., 2016; Platis et al., 2018). In order to assess the realism of the advective transport rates estimated by our hydrodynamic setup, we are planning to do a comparison with other models, such as the operational model of the BSH (see Callies et al., 2017).

Despite these limitations the potential imperfections in the representation of hydrodynamical processes, the model was able to reproduce various characteristic features of the system, as indicated by the low bias and high correlation coefficients in general (e.g., Fig. 5) for temperature, salinity and nutrients (e.g., Figs. 5, 6, 8). The skill of the model in reproducing chlorophyll concentrations was not as good (Fig. 8, see below for a discussion of potential reasons). Importantly, the influence of the meteorological and hydrological peculiarities on the hydrodynamical (Figs. 6, 7, A1) and biogeochemical structure of the system were captured (Figs.8, 9, 14).

The skill of the model at the Helgoland station, both with respect to the physical (Fig.6) and biogeochemical variables (Fig.8) is notable noteworthy, given the heterogeneities caused by the complex topography, and the sharp gradients around the island (Callies and Scharfe, 2015) ., owed to its location at a coastal transition zone. For instance, the sharp DIN peak observed and simulated at Helgoland during June/July 2013 is uncommon for the summer season (see (Voynova et al., 2017), Fig. 12). Overlapping DIN and freshwater fronts simulated by the model, temporarily spreading to the west of Helgoland during the same period (not shown), and supported also by a sharp decline of observed and simulated salinities (6), reveal that this rare summer DIN peak was caused by the plume of the Elbe-Weser flood. This provides evidence for the model's ability to reproduce the behavior of the plume.

We conclude that the model can be used for an exploratory analysis to gain a better understanding of the role of riverine and meteorological forcing in shaping of the hydrodynamical and biogeochemical structure of the German Bight.

Since the first 3D models of the North Sea (Backhaus, 1985; Dippner, 1993; Schrum, 1997), computational capacity has been significantly improved, which resulted in development of ever finer resolution setups that can resolve meso-scale features such as the coastal freshwater fronts and baroclinic eddies (Holt and James, 2006; Pohlmann, 2006; Staneva et al., 2009; Pätsch et al., 2017) and the smaller-scale dynamics, such as the estuarine mixing (Gräwe et al., 2016; Stanev et al., 2019). For large-domain biogeochemical applications that require a costly calculation of transport of dozens of additional state variables, the coarse-resolution models (10-20 km) are being actively used (e.g., Ford et al., 2017; Große et al., 2016; Daewel et al., 2019). With a spatial resolution of 1.5-4.5 km covering the southern North Sea (Fig. 1), the setup we employed here falls somewhere in the middle of the spectrum, and is similar to the setup used by Los et al. (2008) and the 'southeastern North Sea' setup of Androsov et al. (2019). Based on a 144-node setup on the Mistral-phase 2 HPC environment (https://www.dkrz.de/en-pdfs/en-docs/en-docu-mistral/en-mistral_user-manual.pdf), computational cost of the full, coupled model system (i.e., with the biogeochemical model with 25 pelagic state variables, Fig.2) is about 360 CPUh/year (approximate speed-up (simulated time interval over duration of simulation) of 3500), while that of the uncoupled physical model is about 80 CPUh/year (approximate speed-up of 16000). Thus, the setup is suitable for performing coupled physical-biogeochemical simulations or scenario analyses with multi-annual or even decadal time scales.

4.2 Physical and biogeochemical structure of the system

Based on a plethora of *in-situ* observations, Voynova et al. (2017) reported a number of anomalies in the German Bight, following the historical flood event in June 2013, during which, a large quantity of freshwater and nutrients were delivered to the coast by the Elbe and Weser rivers within a short time period (Fig. 3). Our numerical simulations are in agreement with many of those findings, such as the anomalous spatial distribution of salinity, nitrogen and silicate following the flood event (e.g., compare Fig. 10, 12 with the Fig. 11 of Voynova et al. (2017)).

In addition, our findings point to the relevance of the meteorological conditions that interact with the impacts of the flood event. In particular, our findings suggest that mainly the wind conditions (Fig. 4) resulted in a particularly intense stratification (Fig.11). Within the central German Bight, a combination of thermal and haline dynamics extended the area of intense stratification. The thermohaline dynamics in the inner German Bight have been recognized before (Frey, 1990; van Leeuwen et al., 2015). Following the flood event, these interactions have moved away from the coast to further offshore regions of the German Bight. It should be noted that, variations in stratification intensity driven by the spring and neap tides as in the Rhine ROFI (Simpson et al., 1993) have been identified for our study system as well, but these are relevant at shorter (weekly) time scales (Chegini et al., submitted).

The enhanced water column stability (Fig. 11), and hence reduced light limitation, in combination with higher nutrient availability supplied by the flood event (Fig. 3, 12), increased the NPPR within the central German Bight (Fig. 12), which may explain the high pH and DO oversaturation reported by Voynova et al. (2017). In turn, the combination of ~~prolonged stratification~~ uninterrupted phases of stratification during July that gave rise to a large average density difference (Fig. 11) and the breakdown of high amounts of organic material as a result of enhanced NPPR (Fig. 12), following the flood event, lead to a widespread oxygen depletion in the bottom layers. The DO supersaturation ~~at the surface and bottom~~ in the surface layers, and subsequent ~~subsaturation~~ undersaturation in bottom waters observed in the Deutsche Bucht station, which was previously documented by Voynova et al. (2017), was correctly captured by the model (Fig.14). The scenario analysis suggests that,

especially the meteorological conditions during the summer of 2013, but also the flood event were relevant for the occurrence and intensity of this oxygen drawdown in the German Bight (Fig. 13-14). This explains why such a degree of oxygen depletion in the German Bight is unusual (e.g., Voynova et al., 2017; Große et al., 2016, 2017). Within the outer German Bight, the higher water column stability lead to an intensification of the nutrient limitation within the upper mixed layer, and consequently lower NPPR (Fig. 12). At the vicinity of the ~~mouth of Elbe-Weser~~ **mouths of the Elbe and Weser** rivers, NPPR ~~does~~ **did** not respond strongly to the flood (Fig. 12), as these areas ~~are more~~ **were** limited by light, rather than nutrients (see also Loebl et al., 2009). In reality, an even stronger light limitation in the vicinity of the mouth of the Elbe estuary is likely, due to the increase in the SPM towards the Elbe estuary (van Beusekom and Brockmann, 1998; Gayer et al., 2006), which is only partially accounted for by the model (see Appendix B2). It should be noted that the riverine influence within the coastal zone may be overestimated by our simulations, given the lower than observed salinities (Fig. 7), and higher than observed nutrient concentrations (Fig. 9).

Our results point to an increase in current velocities at the surface under the influence of the 2013 flood (Fig. 15), which is presumably driven by the reduced dissipation of kinetic energy through vertical mixing, owed to the intensification of haline stratification (Fig. 11), i.e., the baroclinicity of the current structure. Enhancement of the current velocities at the surface, in turn, might have facilitated the spread of the plume towards the outer German Bight in 2013 (Fig.10-12). However, the main reason for the eastward spread of the plume is the wind conditions, which presumably lead to a dominance of anticyclonic circulation during July 2013, as **was** also suggested by a principal component analysis of a barotropic model simulation (https://coastmap.hzg.de/coastmap/modeldata/model1/#/residualcurrents, see Callies et al. (2016) for data access). It has been ~~earlier~~ shown that the residual surface currents in the German Bight are largely determined by the wind patterns (Schrum, 1997; Callies et al., 2017).

van Beusekom et al. (2019) ~~had earlier showed~~ **has shown** and discussed the presence **of** regional differences in thermohaline estuary-type circulation (as in Burchard and Badewien, 2015; Hofmeister et al., 2017) in the Wadden Sea. Here, our results suggest that the strength of the thermohaline estuarine circulation (Burchard and Badewien, 2015) can be enhanced by surplus buoyancy fluxes, here driven by the flood event (Fig. 16), ~~which~~ . **This** is as expected, and can enhance coastal accumulation of SPM and nutrients even ~~distant to~~ **away from** the estuary itself (Hofmeister et al., 2017).

Our model-based analysis here is not conclusive, but rather exploratory. Given the anticipated increase in the frequency and intensity of the hydro-meteorological extremes due to climate change (Beniston et al., 2007; Wetz and Yoskowitz, 2013), further research is needed to understand the processes underlying the interactive impacts of these events on the physical and biogeochemical structure of the coastal systems and estuaries. Such a mechanistic understanding is essential for policy making, such as the regulation of nutrient loading rates in rivers (see, e.g., OSPAR, 2017).

4.3 Model limitations and perspectives

Since the first 3D models of the North Sea (Backhaus, 1985; Dippner, 1993; Schrum, 1997), computational capacity has been significantly improved, which resulted in development of ever finer resolution setups that can resolve meso-scale features such as the coastal freshwater fronts and baroclinic eddies (Holt and James, 2006; Pohlmann, 2006; Staneva et al., 2009; Pätsch et al., 2017), and smaller-scale dynamics, such as the estuarine processes (Gräwe et al., 2016;

Stanev et al., 2019; Pein et al., 2019). For large-domain biogeochemical applications that require a costly calculation of transport of many additional state variables, the coarse-resolution models (10-20 km) are being actively used (e.g., Große et al., 2016; Ford et al., 2017; Daewel et al., 2019). With a spatial resolution of 1.5-4.5 km covering the southern North Sea (Fig. 1), the setup we employed here falls in the middle of the spectrum, and is similar to the setup used by Los et al. (2008) and the 'southeastern North Sea' setup of Androsov et al. (2019).

A potential source of bias in salinity and nutrients along the Elbe-plume is the misrepresentation of the Elbe estuary in our model setup (Fig. 1). For instance, according to a recent, high resolution model of the Elbe estuary, the freshwater-saline water transition (0-5 g/kg) occurs at about 50-75 km upstream of the mouth of Elbe (under normal hydrological conditions), and the N and Si concentrations vary considerably within the estuary (Pein et al., 2019). Indeed, a high resolution (300m) setup of the German Bight that resolves up to 150 km upstream the Elbe mouth (Chegini et al., submitted) demonstrated better skill in reproducing the salinity observations shown in Fig.7 and Fig. A1. Another contingent error source is potential inaccuracies in advective transport rates, e.g., as a result of imperfections in meteorological forcing (Geyer, 2014); or ignoring the effects of off-shore wind-farms on the thermohaline circulation (Carpenter et al., 2016; Platis et al., 2018). In order to assess the realism of the advective transport rates estimated by our hydrodynamic setup, we are planning to do a comparison with other models, such as the operational model of the BSH (see Callies et al., 2017).

The structure and process descriptions used for the biogeochemical model introduced in this study are similar to those used recently for studying the interaction between the hydrodynamical and biogeochemical processes in coastal systems, in particular, nutrient cycling and oxygen dynamics, in the North Sea (e.g. Große et al., 2016; Kerimoglu et al., 2017a), the Elbe estuary (Pein et al., 2019) and other similarly dynamic coastal shelf systems, such as the Louisiana Shelf (Fennel and Laurent, 2018) and the Chesapeake Bay (Irby et al., 2018). Description of the non-planktonic components, consisting of two detritus classes, dissolved organic material, dissolved inorganic nutrients, oxygen, and a simple benthic pool to represent benthic remineralization, oxygen consumption and denitrification (Fig. 2) were largely based on ECOHAM (see Section 2.1 Appendix B), which was earlier derived from ERSEM. Unlike ECOHAM, but like in a majority of the aforementioned models (Feng et al., 2015; Kerimoglu et al., 2017a; Laurent et al., 2017; Pein et al., 2019), DOM remineralization is described as first order kinetics, instead of mediated by an explicitly described bacteria, which, considering the purposes of the model, we consider to be non-critical. Underestimated oxygen depletion (Fig. 14), and the inability of the model to capture some high P concentrations (reflected as sporadic, but large underestimation errors in Fig. 5), are possibly related to the oversimplifications in the benthic model, which is, again, a weakness shared by a majority of the aforementioned model studies. Simulated benthic oxygen consumption rates of up to 15 mmol m^{-2} d^{-1} during the summer months is less than half of the upper range of measurements in the German Bight (e.g. Ahmerkamp et al., 2017). The foremost reason for this underestimation is likely the inaccuracies in POM deposition rate as determined by the prescribed sedimentation rates of detritus in our model (Table B8). Deposition rate is, in reality, increasingly recognized to be controlled by the spatially heterogeneous sediment permeability (Ahmerkamp et al., 2017) and microalgal/macrofaunal activity in the benthos (Middelburg, 2018). The lack of an explicit representation of the benthic oxygen profiles and redox reactions may

have contributed to the problem, although it was shown that a vertically integrated approximation like the benthic model we used, especially when combined with meta-model parameterizations, can reliably behave like a computationally demanding, vertically resolved explicit diagenetic model (Soetaert et al., 2000). The sporadic large underestimation errors in P concentrations are identified to occur in some coastal regions during summer months, when the nitrogen concentrations are at their lowest. Such decoupling of phosphorus and nitrogen in certain Wadden Sea regions is well known, and recognized to be driven by the depletion of benthic oxygen during summer, which leads to release of iron-bound P, while promoting denitrification in the sediments (see, e.g. Loebl et al., 2007; Grunwald et al., 2010; Leote et al., 2015). Although the latter is accounted for by our model (Table B8), the former is not, which can explain the inability of the model in capturing the late-summer P peaks.

In three out of four stations we considered, chlorophyll concentrations are overestimated (Fig. 8). Considering these biases, rather than the absolute values of NPPR estimates, simulated responses to hydro-meteorological forcing should be regarded (Fig. 12). Reasons for the overestimation of chlorophyll concentrations seem to be region specific: overestimation of winter concentrations in Terschelling-50 and Noordwijk-70 suggest insufficient respiration rates, whereas spring blooms starting too early at Helgoland suggest inaccuracies in the seasonality of under-water light climate. During the summer months, misrepresentation of grazing losses and vertical distribution of chlorophyll (e.g., van Leeuwen et al., 2013; Kerimoglu et al., 2017a) may have contributed to the overestimation errors as well. A detailed identification of the chlorophyll dynamics therefore require a careful consideration of all these factors and comparisons against additional datasets, which is out of the scope of this study. However, differences in baseline concentrations at different stations during summer are quite realistically reproduced, suggesting that the large-scale gradients are realistically represented (Fig. 8), which we consider to be sufficient for the purposes of this study. The structure of the plankton food web assumed in this study, consisting of two phytoplankton (flagellates and diatoms) and two zooplankton (micro- and mesozooplankton) groups, is similar to those by Große et al. (2017) and Pein et al. (2019), but here the variability in phytoplankton cellular composition were taken into account, using the Droop and Geider et al. (1997) formulations to resolve the variability in C:N:P and Chl:C, respectively, similar to as in, e.g., ERSEM (e.g., Ford et al., 2017). In the future, we are planning to improve the representation of other plankton groups in the system, such as colony-forming *Phaeocystis* and mixotrophic forms, which can be abundantly found in the coastal waters of the southern North Sea (Löder et al., 2012; Burson et al., 2016). A module that provides a simplistic description of mixotrophy (as in Kerimoglu et al., 2017b), is already available, but we chose not to use it in this study, for the sake of avoiding increasing the model complexity further.

Given the limitations of the biogeochemical model discussed above, its predictions should not be interpreted in an absolute sense. However, the model structure and formulations represent the state of the art, and the simulated responses by the model are plausible. Therefore the analysis presented in this study is of heuristic value in gaining a systematic understanding of the role of riverine and meteorological forcing in shaping of the hydrodynamical and biogeochemical structure of the system.

5 Conclusions

In this study, we presented a newly developed biogeochemical model and improvements of a hydrodynamical model described in an earlier study. The coupled hydrodynamical-biogeochemical model system is shown to satisfactorily reproduce the characteristic features of the German Bight ecosystem, and the impacts of a 100-year flooding of the Elbe and Weser rivers. Our results reveal that the flood event coincided with special meteorological conditions in the region, namely a calm and warm summer dominated by an anticyclonic circulation, resulting in a particularly intense and widespread stratification. The stronger stratification, and the increased availability of nutrients impacted the primary production in the system and the oxygen levels ~~at~~ in the bottom waters. Through a scenario analysis, we found ~~out~~ that the observed anomalies in July 2013 were likely driven by ~~both~~ the meteorological conditions within the outer German Bight, and ~~their interaction~~ the interaction between meteorological and hydrological conditions within the central German Bight, suggesting that the impacts of ~~the~~ flood events in the system are context-dependent. These extreme flooding and meteorological conditions may occur more frequently in the future, which requires a better understanding of the mechanisms governing the response of the coastal systems to such extreme events.

Appendix A: Description of horizontal diffusion in the hydrodynamical model

Modern advection schemes (including TVD-transport as used in many coastal applications) are developed and tested for homogeneous grid spacing (Pietrzak, 1998; Barthel et al., 2012), although coastal applications tend to use varying grid spacing in curvilinear horizontal, unstructured horizontal and general vertical grids (e.g., Zhang et al., 2016; Kerimoglu et al., 2017a). The performance of slope limiters and the involved numerical mixing is therefore almost unpredictable for two reasons: a) tracer mixing is ultimately always a combination of numerical mixing and physical mixing terms, both effects reduce each other (Hofmeister et al., 2011), and b) numerical mixing as a nonlinear effect of the advection is seldom analyzed in model applications. Comparisons of the mixing term strength between model applications then potentially result in differences of the advection scheme performance, more than an analysis of the physical effect of mixing mass concentrations.

There exists a plethora of methods for the specification of horizontal diffusion or isopycnal mixing for ocean models (see, e.g. Gent and McWilliams, 1990; Roberts and Marshall, 1998; Beckers et al., 2000; Griffies and Hallberg, 2000), a review or discussion of which is beyond the scope of this appendix. Here, we will demonstrate the use of a simple subgridscale parameterization by Smagorinsky (1963), which was originally for modelling atmospheric circulation, and is now commonly used in both atmospheric and ocean circulation models (Becker and Burkhardt, 2007). The magnitude of horizontal diffusivity is recognized to exhibit strong variations in space and time (Wang, 2003). The Smagorinsky parameterization achieves such variations by scaling the diffusion coefficient proportionally with the grid size and deformation rates of lateral velocities, e.g., for the horizontal diffusion of momentum:

$$A_M = C_S * \Delta x \Delta y * \sqrt{\left(\frac{\partial u}{\partial x}\right)^2 + \left(\frac{\partial v}{\partial y}\right)^2 + \frac{1}{2}\left(\frac{\partial u}{\partial y} + \frac{\partial v}{\partial x}\right)^2} \tag{A1}$$

where, C_S is the empirical Smagorinsky constant, u, v, Δx and Δy are velocities and grid spacings along x and y dimensions, respectively. Then the horizontal diffusion of tracers, A_H follows:

$$A_H = A_M / Prt \tag{A2}$$

In (A1), C_S is not physically well constraint, but is adjusted based on numerical considerations (Kantha and Clayson, 2000), e.g., the diffusion vs. dispersion trade-off (Pietrzak, 1998). In this study, we set $C_S = 0.6$ and Prandtl number, $Prt = 1.0$, and examine the effects of this parameterization on the representation of the river plume during 2012-2013, with a focus on the freshwater plume during the flooding event. Specifically, we compare the predictions of 2 model variants against the Ferrybox measurements taken by the platform installed on the M/V *Funny Girl* ferry, that are analyzed in greater detail in the main text (Fig. 7).

The variant where no diffusion was enabled, overestimates the cross-shore salinity gradient along the North Frisian coast, i.e., North of Elbe, in the form of too low near-coast salinities (Fig.A1b). On the other hand, the variant where horizontal diffusion was described with Smagorinsky parameterization, have considerably better skill in reproducing the FerryBox measurements along the Büsum-Helgoland ferry track (Fig. A1c).
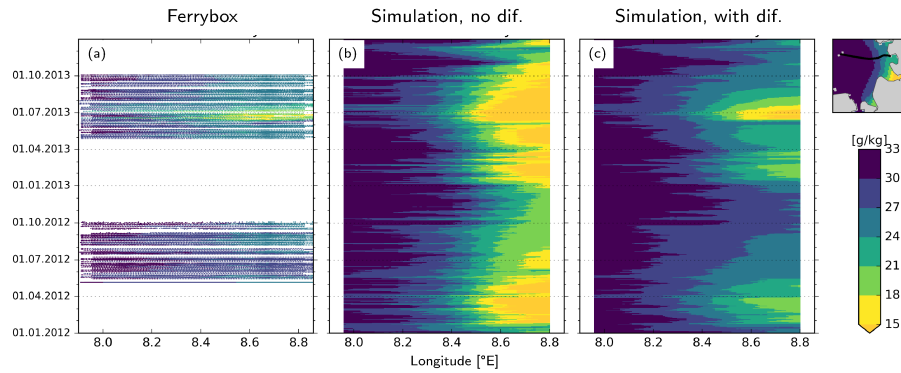
Figure A1. Hovmöller diagrams of salinity distribution in 2012 and 2013 along the (average) transect shown at the top right corner, as measured by the FerryBox platform (a) and models without (b) and with (c) horizontal diffusion.

Plausibility of the total horizontal mixing, and its physical and numerical components can be diagnosed by an analysis of the discrete variance decay (DVD) of salinity (Klingbeil et al., 2014) based on Burchard and Rennau (2008). In the absence of explicit diffusion, the sum of physical and numerical mixing becomes negative at the mouth of the Elbe and Weser rivers, and within their ROFI, implying spuriously enhanced horizontal gradients (Fig. A2c). With the application of explicit diffusion,
555   numerical mixing values effectively decrease both within the positive and negative spectra (Fig. A2d), leading to near-complete elimination of negative values of the total mixing being removed in total mixing (Fig. A2f).
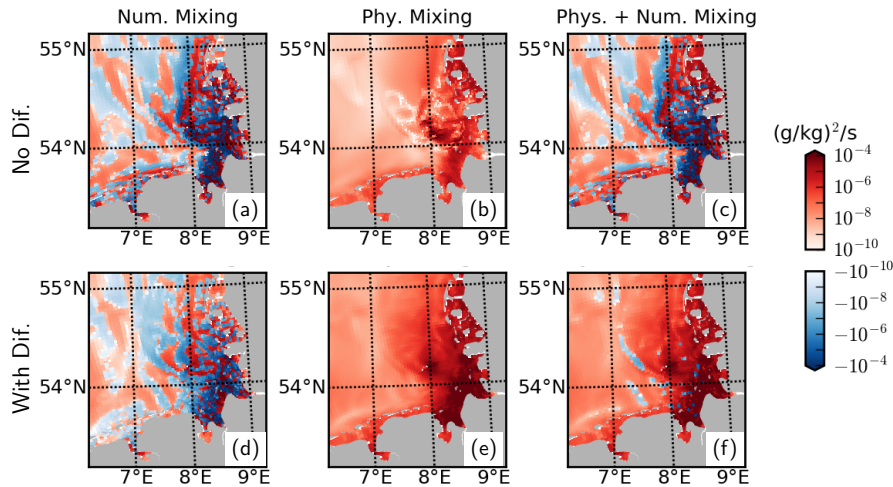
Figure A2. Mixing analysis for July 2013 based on temporally averaged values at the surface.

We conclude that application of explicit horizontal mixing through a simple parameterization can be useful in improving the skill of a 3-D coupled physical-biogeochemical model within the vicinity of river discharges, and eliminate implausible negative total (physical + numerical) mixing values.

Appendix B: Detailed description of the biogeochemical model

All modelled state variables and fluxes between various pools are shown in Fig. 2. In the following sections, sink and source terms for the planktonic and abiotic variables ($s(v)$ in Tables B1, B7) and the description of processes (Tables B2, B4, B9) will be provided. For describing the fluxes between various pools, where possible, we adopt the $source\_target$ notation as in Pätsch and Kühn (2008), which was earlier adopted from ERSEM (Blackford and Radford, 1995). Although this notation is consistent with that used in the Fortran ~~program~~ module of abiotic components, the programming notation of the ~~Planktonic components~~ ~~are~~ plankton module is somewhat different, due to their different historical origins.

All kinetic rates in planktonic and abiotic components are modified with temperature using the Q10 rule:

$$f_{T,(phy,zoo-j,abio)} = Q10_{(phy,zoo-j,abio)}^{(T-T_{ref})/T_{ref}} \tag{B1}$$

with $T_{ref} = 10°C$, and $Q10_{phy} = Q10_{zoo-mic} = Q10_{abio} = 1.5$ and $Q10_{zoo-mes} = 2.0$.

B1 Planktonic components

The plankton model was developed based on Kerimoglu et al. (2017b) regarding the modularity concept that allows coupling plankton units in run time (see Bruggeman and Bolding, 2014), as well as description of internal variation of P quota of phytoplankton (B2,B4,B12) according to the Droop model (as in Morel, 1987). Here, we further considered the uptake ~~NO3 and NH4~~ NO_3 and NH_4 of phytoplankton (similar to Pätsch and Kühn, 2008), and the resulting variations of N quota (B3,B13); limitation of diatoms by Si (B11) using a Monod-type relationship (Flynn, 2003); dependence of the light limitation on the chlorophyll content, i.e., θ (B15), in phytoplankton (B9), and the dynamic variations of θ (B5,B16) following Geider et al. (1997). The plankton module provides various options for the representation of nutrient and carbon limitation in a consistent way, which is intended to be further enriched and elaborated in future studies. Given the suppleness of the model with respect to the description of physiological processes and interactions between species, the model is provisionally named as the 'Generalized Plankton Model' (GPM).

Table B1. Source-sink terms of the dynamic variables (all in mmol/m³/d) of the plankton module. Indices p_i= {diatoms, ~~nanoflagel-lates~~flagellates}; z_j={microzooplankton, mesozooplankton}; t_k= zooplankton target.

C bound to p_i	$s(p_i^C)$	$= DIC\_p_i^C - p_i^C\_DOC - M_i^C - \sum_j I_{j,i}^C \cdot z_j^C$	(B2)
N bound to p_i	$s(p_i^N)$	$= NO3\_p_i^N + NH4\_p_i^N - p_i^N\_DON - M_i^N - \sum_j I_{j,i}^N \cdot z_j^C$	(B3)
P bound to p_i	$s(p_i^P)$	$= DIP\_p_i^P - p_i^P\_DOP - M_i^P - \sum_j I_{j,i}^P \cdot z_j^C$	(B4)
Chl bound to p_i	$s(p_i^{chl})$	$= \rho_i \cdot DIC\_p_i^C - (p_i^C\_DOC + M_i^C + \sum_j I_{j,i}^C \cdot \theta_i \cdot 12.0[gC/molC] \cdot z_j^C$	(B5)
C bound to z_j	$s(z_j^C)$	$= \sum_k t_k^C\_z_j^C - zC_j\_DIC - M_j^C$	(B6)

As in Kerimoglu et al. (2017a), sinking rate of phytoplankton is formulated as a function of their nutrient status.

$$w_{p,i} = w'_p \cdot \left(0.1 + 0.9 \cdot \exp\left(-5.0 * \min\left(\frac{QP_i - QP_{min,i}}{QP_{max,i} - QP_{min,i}}, \frac{QN_i - QN_{min,i}}{QN_{max,i} - QN_{min,i}} \right) \right) \right) \tag{B7}$$

In (B7) and in Tables B1-B2, $QX = X : C$ within a certain phytoplankton or zooplankton pool, which may be either a fixed constant (as provided in Table B3), or diagnostically calculated from the instantaneous values (for $X = P, N$ quota of phytoplankton). Exudates of the phytoplankton are assumed to be in DOM form (B2,B17).

Table B2. Process equations and functional relationships used in the phytoplankton module

C uptake rate of p_i	$DIC\_p_i^C$	$= p_i^C \cdot f_{T,phy} \cdot V_{max,i}^C \cdot f_{I,i} \cdot \min(f_{N,i}, f_{P,i}, f_{Si,i})$	(B8)
Light limitation of p_i	$f_{I,i}$	$= 1.0 - \exp\left(\frac{-\alpha_i \cdot \theta_i \cdot I}{f_{T,phy} \cdot V_{max,i}^C \cdot \min(f_{N,i}, f_{P,i})} \right)$	(B9)
Nutrient (X={N,P}) limitation of p_i	$f_{X,i}$	$= 1.0 - QX_{min,i}/QX_i$	(B10)
Silicate limitation of diatoms	$f_{Si,i}$	if $i : diatoms = \frac{DISi}{K_i^{Si} + DISi}$, else $= 1.0$	(B11)
DIP uptake rate of p_i	$DIP\_p_i^P$	$= p_i^C \cdot f_{T,phy} \cdot V_{max,i}^P \cdot \frac{QP_{max,i} - QP_i}{QP_{max,i} - QP_{min,i}} \cdot \frac{DIP}{K_i^P + DIPi}$	(B12)
DINX (NX={NO3,NH4NO$_3$,NH$_4$}) uptake rate of p_i	$DIX\_p_i^N$	$= p_i^C \cdot f_{T,phy} \cdot V_{max,i}^N \cdot \frac{QN_{max,i} - QN_i}{QN_{max,i} - QN_{min,i}} \cdot \frac{DINX/K_i^{NX}}{1.0 + \sum_X DINX/K_i^{NX}}$	(B13)
Silicate uptake rate of p_i	$DISi\_p_i^{Si}$	if $i : diatoms = DIC\_p_i^C \cdot QSi_i$, else $= 0.0$	(B14)
Chl:C ratio bound to p_i	θ_i	$= p_i^{chl}/(p_i^C \cdot 12[gC/molC])$	(B15)
Ratio of chl. synthesis to C fixation	ρ_i	$= \frac{DIC\_p_i^C/p_i^C}{\alpha_i \cdot \theta_i \cdot I}$	(B16)
X (=C,N,P) exudation of p_i	$p_i^X\_DOX$	$= DIC\_p_i^C \cdot \gamma_i \cdot QX_i$	(B17)
X (=C,N,P) Mortality rate of p_i	M_i^X	$= p_i^X \cdot f_{T,phy} \cdot (m1_i + p_i^C \cdot m2_i)$	(B18)

Process formulations for the zooplankton module are provided in Table B4. Following Fasham et al. (1990), prescribed preferences of prey items for each zooplankton (Table B6) are dynamically weighed with their relative abundance to determine the effective preferences (B26,B27). Zooplankton are assumed to excrete into DIM pool (B6,B24).

As in Kerimoglu et al. (2017b), assimilated and un-assimilated fractions of the ingested prey by each zooplankton j are determined by the assimilation efficiency ϵ_j^X (B28),B29), which is continuously adjusted (as in Grover, 2002), such that the zooplankton can maintain their homeostatic elemental composition. Here this scheme was extended to multiple nutrients, i.e., N and P, and ϵ^X are calculated iteratively, similar to that in (Kerimoglu et al., 2018). Starting from each ϵ^X set to default values (Table B5), if P to be ingested would be less than the amount required to match the ingested C, ϵ^C is down-regulated, and vice versa:

$$\epsilon^P = \frac{\epsilon_j^C \cdot \sum_k I_{j,k}^C \cdot QP_j}{\sum_k I_{j,k}^P}, \quad \text{if } \epsilon_j^P \cdot \sum_k I_{j,k}^P > \epsilon_j^C \cdot \sum_k I_{j,k}^C \cdot QP_j \tag{B19}$$

$$\epsilon^C = \frac{\epsilon_j^P \cdot \sum_k I_{j,k}^P}{\sum_k I_{j,k}^C \cdot QP_j}, \qquad \text{otherwise} \tag{B20}$$

Table B3. Parameters of the phytoplankton module. Where necessary, multiple values were provided for diatoms and ~~nanoflagellates~~flagellates.

Sources: G98: based on Geider et al. (1998); K17: Kerimoglu et al. (2017b); L12: Lorkowski et al. (2012); A: assumed; C: calibrated.

Symbol	Description	Value$_i$	Unit	Source
$V_{\mathrm{max,i}}^{C}$	Maximum C uptake rate	3.0, 2.0	d^{-1}	G98
$V_{\mathrm{max,i}}^{N}$	Maximum N uptake rate	0.3, 0.6	molN (mmolC d)$^{-1}$	G98
$V_{\mathrm{max,i}}^{P}$	Maximum P uptake rate	0.01, 0.02	molP (mmolC d)$^{-1}$	A
K_i^{NO3}	Half saturation constant for ~~NO3~~ NO_3 uptake	3.0	mmolN m^{-3}	G98
K_i^{NH4}	Half saturation constant for ~~NH4~~ NH_4 uptake	1.0	mmolN m^{-3}	A
K_i^{P}	Half saturation constant for P uptake	0.4	mmolP m^{-3}	K17
K_i^{Si}	Half saturation constant for Si limitation	1.0	mmolSi m^{-3}	A
$QS_{i\mathrm{diat}}$	Fixed Si:C ratio of diatoms	0.17 ,0.0	molSi molC^{-1}	L12
$QN_{\mathrm{max,i}}$	Maximum quota for N	0.18	molN molC^{-1}	G98
$QP_{\mathrm{max,i}}$	Maximum quota for P	0.008	molP molC^{-1}	A
$QN_{min,i}$	Subsistence N quota	0.045, 0.06	molN molC^{-1}	G98
$QP_{min,i}$	Subsistence P quota	0.002, 0.003	molP molC^{-1}	A
α_i	Chl. sp. slope of P-I curve	9.0, 6.0	gC gChl^{-1} / (molE m^{-2})	G98
w_p'	Maximum potential sinking rate	4.0,0.2	m d^{-1}	
$\theta_{max,i}$	Max. chl:C ratio	0.10, 0.07	m^2 gChl/gC^{-1}	A
γ_i	Exudation fraction	0.05	-	L12
$m1_i$	Linear mortality rate	0.05	d^{-1}	C
$m2_i$	Quadratic mortality rate	0.001	d^{-1}/(mmolC m^{-3})	C
$\delta_{S,i}$	Fraction of dead cells diverted to small det.	0.7,1.0	-	L12
w_p'	Maximum potential sinking rate	4.0, 0.2	m d^{-1}	C

Next, following the same logic, ϵ^N and ϵ^C are regulated to match the C- and N-intake according to the QN_j:

$$\epsilon^N = \frac{\epsilon_j^C \cdot \sum_k I_{j,k}^C \cdot QN_j}{\sum_k I_{j,k}^N}, \quad \text{if } \epsilon_j^N \cdot \sum_k I_{j,k}^N > \epsilon_j^C \cdot \sum_k I_{j,k}^C \cdot QN_j \tag{B21}$$

$$\epsilon^C = \frac{\epsilon_j^N \cdot \sum_k I_{j,k}^N}{\sum_k I_{j,k}^C \cdot QN_j}, \qquad \text{otherwise} \tag{B22}$$

600   Finally, ϵ^P is adjusted again, as a potential modification of ϵ^C in (B21) may require an updated P-intake:

$$\epsilon^P = \frac{\epsilon_j^C \cdot \sum_k I_{j,k}^C \cdot QP_j}{\sum_k I_{j,k}^P}, \quad \text{if } \epsilon_j^P \cdot \sum_k I_{j,k}^P > \epsilon_j^C \cdot \sum_k I_{j,k}^C \cdot QP_j \tag{B23}$$

Table B4. Process equations and functional relationships used in the zooplankton module.

X (=C,N,P) Excretion rate of z_j	$z_j^X\_DIX$	$= z_j^C \cdot e_j \cdot f_{T,zoo-j} \cdot QX_j$	(B24)
X (=C,N,P) Mortality rate of z_j	M_j^X	$= z_j^C \cdot (m1_j + z_j^C \cdot m2_j) \cdot QX_j$	(B25)
Ingestion rate of X from t_k	$I_{j,k}^X$	$= I_{max,j} \cdot f_{T,zoo-j} \cdot \frac{pw_{j,k} \cdot t_k^C}{K_j^C + \sum_k (pw_{j,k} \cdot t_k^C)} \cdot QX_k$	(B26)
Weighed preference of target k by j	$pw_{j,k}$	$= pref_{j,k} \cdot t_k^C / \sum_k (pref_{j,k} \cdot t_k^C)$	(B27)
Assimilated X={C,N,P,Si} ingestion of	$t_k^X\_z_j^X$	$= z_j^C \cdot \epsilon_j^X \cdot I_{j,k}^X$	(B28)
Total unass. X={C,N,P,Si} ing. by z_j	U_j^X	$= z_j^C \cdot \sum_k \cdot (1 - \epsilon_j^X) \cdot I_{j,k}^X$	(B29)

Table B5. Parameters of the zooplankton module. Where necessary, multiple values were provided for micro- and meso-zooplankton.Sources: H97: based on the range provided by Hansen et al. (1997); S97: based on Straile (1997); K17: Kerimoglu et al. (2017b); L12: Lorkowski et al. (2012); RF: Redfield ratio; A: assumed; C: calibrated.

Symbol	Description	Value$_j$	Unit	Source
$I_{max,j}$	Maximum ingestion rate	1.8, 1.5	-	H97
K_j^C	Half saturation constant	15.0, 20.0	-	H97
Q_j^N	Constant N:C ratio of z_j	0.15	molN molC^{-1}	RF
Q_j^P	Constant P:C ratio of z_j	0.0094	molP molC^{-1}	RF
ϵ_j^C	C Assimilation efficiency	0.5, 0.4	-	S97
$\epsilon_j^{N,P}$	N&P Assimilation efficiency	0.8, 0.8	-	A
e_j	Excretion rate	0.05	d^{-1}	A
$m1_j$	Linear mortality rate	0.02	d^{-1}	C
$m2_j$	Quadratic mortality rate	0.01, 0.02	d^{-1}/(mmolC m^{-3})	C
$\delta_{S,j}$	Fraction of mort. & unass. ing. diverted to small det.	0.85, 0.7	-	L12
δ_{dom}	Fraction of DOM in unassimilated ingestion	0.8	-	A

Table B6. Grazing Assumed grazing preferences $pref_{j,k}$ of predator j (rows) for target t_k (columns).

	det_S	p_{nf} p_{flag}	p_d p_{diat}	z_{mic}
z_{mic}	0.4	0.5	0.1	-
z_{mes}	-	0.3	0.1	0.6

B2 Abiotic component

B2.1 Organic material and nutrients

The abiotic components, describe the geochemical transformation between various organic and inorganic pools (DIM, DOM, small and large detritus classes, O_2 and the particulate organic matter in the benthos (B-POM), see Fig. 2). Model structure used here is simplified from ECOHAM (Lorkowski et al., 2012), by excluding carbonate and bacterial dynamics entirely and simplifying the description of DOM remineralization. The latter is described here as a first order kinetic reaction (eq. B43), instead of a more detailed description of scavenging of DOM by bacterial biomass in the original model. Coupling of the abiotic component with the planktonic components are mediated through the uptake of DIM by phytoplankton (B3,B4), and the recycling of the dead and surplus material. The unassimilated fraction of the ingestion by zooplankton are distributed into the DOM (B35) and the two detritus pools as in Lorkowski et al. (2012). For X=C,N,P, mortality of plankton (B18,B25) are distributed into the small and large detritus classes (B36,B37). For Si, there are no DOM or det_S^{Si} pools (Fig.2), therefore all diatom mortality and Si bound to the ingested diatoms are diverted to the det_L^{Si} (B38).

Conversion of areal units (mmolX/m^2/d) of the surface and bottom flux terms (B52-B56) to volumetric units (mmolX/m^3/d) required for the pelagic variables is handled by the FABM coupler through division by the surface and bottom layer thicknesses ($\Delta z(s)$, $\Delta z(b)$) internally, which are specified here but not in the model codes.

Table B7. Source-sink terms of the dynamic variables (all in mmol/m^3/d, except for the benthic variables (B39-B40) in mmol/m^2/d) of the abiotic module. Description of processes or functional relationships and parameters are provided in Tables B9 and B8, respectively.

DINO3	$s(DINO3) = DINH4\_DINO3 - \sum_i DINO3\_p_i^N - DINO3\_BPOM/\Delta z(b) - DINO3\_N2$	(B30)
DINH4	$s(DINH4) = BPON\_DINH4/\Delta z(b) + DON\_DINH4 + sum_j z_j^N\_DIN - \sum_i DINH4\_p_i^N - DINH4\_DINO3$	(B31)
DIP	$s(DIP) = BPOP\_DIP/\Delta z(b) + DOP\_DIP + sum_j z_j^P\_DIP - \sum_i DIP\_p_i^P$	(B32)
DISi	$s(DISi) = BPOSi\_DISi/\Delta z(b) + det_L^{Si}\_DISi - \sum_i DISi\_p_i^{Si})$	(B33)
O2	$s(O2) = air\_O2/\Delta z(s) + \sum_i p_i\_O2 - \sum_j O2\_z_j - O2\_DOM - O2\_DINH4 - O2\_BPOM$	(B34)
Diss. org. X={C,N,P}	$s(DOX) = \sum_i p_i^X\_DOX + \sum_j (\delta_{dom} \cdot U_j^X) + \sum_{C=S,L} det_C^X\_DOX - DOX\_DIX$	(B35)
Small det. X={C,N,P}	$s(det_S^X) = \sum_i (\delta_{S,i} \cdot M_i^X) + \sum_j (\delta_{S,j} \cdot ((1-\delta_{dom}) \cdot U_j^X + M_j^X) - det_S^X\_DOX - det_S^X\_BPOX/\Delta z(b)$	(B36)
Large det. X={C,N,P}	$s(det_L^X) = \sum_i ((1-\delta_{S,i}) \cdot M_i^X) + \sum_j ((1-\delta_{S,j}) \cdot ((1-\delta_{dom}) \cdot U_j^X + M_j^X) - det_L^X\_DOX - det_L^X\_BPOX/\Delta z(b)$	(B37)
Large det. Si	$s(det_L^{Si}) = \sum_i (M_i^{Si}) + \sum_j U_j^{Si} - det_L^{Si}\_DISi - det_L^{Si}\_BPOSi/\Delta z(b)$	(B38)
Benthic-POX={C,P,Si}	$s(BPOX) = \sum_{c=S,L} det_c^X\_BPOX - BPOX\_DIX$	(B39)
Benthic-PON	$s(BPON) = \sum_{c=S,L} det_c^N\_BPON - BPON\_DINH4 - BPON\_N2$	(B40)

Table B8. Parameters of the abiotic module. Sources: L12: Lorkowski et al. (2012); E5C: ECOHAM5 source code; S96: Seitzinger and Giblin (1996); A: assumed; C: calibrated.

Symbol	Description	Value (C,N,P,Si)	Unit	Source
λ^X	Rem. rate of DOM	0.05	d^{-1}	C
$r_S^{N,P}$	Decay rate of N&P in small det.	0.12	d^{-1}	L12
r_S^C	Decay rate of C in small det.	$r_S^{N,P} \cdot 0.85$	d^{-1}	L12
$r_L^{N,P}$	Decay rate of N&P in large det.	0.1	d^{-1}	L12
r_L^C	Decay rate of C in large det.	$r_S^{N,P} \cdot 0.85$	d^{-1}	L12
$r_L^S i$	Decay rate of Si in large det.	$r_S^{N,P} \cdot 0.085$	d^{-1}	E5C
r_{nit}	Nitrification rate	0.05	d^{-1}	C
QN_b	Bacterial N:C ratio	0.20.25	molN/molC	L12
w_{detS}	Sinking rate of small det.	2.0	$m\ d^{-1}$	C
w_{detL}	Sinking rate of large det.	10.0	$m\ d^{-1}$	L12
br^C	Benthic rem. rate of C	0.028	d^{-1}	L12
$br^{N,P}$	Benthic rem. rate N&P	0.0333	d^{-1}	L12
$br^S i$	Benthic rem. rate of Si	0.0130	d^{-1}	L12
ρ_{Seitz}	Denit./O2 O_2 cons. prop. constant	0.116	molN/molO2O_2	S96
ω_{detS}	Sed. rate of small det.	0.50.25 $\cdot w_{detS}$	$m\ d^{-1}$	C
ω_{detL}	Sed. rate of large det.	5.00.5 $\cdot w_{detL}$	$m\ d^{-1}$	C

B2.2 Light

In GETM, light intensity at a given depth, $I(z)$, is described by:

$$I(z) = I_0 \cdot a \cdot \exp(-\frac{z}{\eta_1}) + I_0 \cdot (1-a) \cdot \exp(-\frac{z}{\eta_2} - \int_z^0 \sum_n K_n(z')dz') \tag{B62}$$

where, I_0 is the light at the water surface, a, η_1 and $\eta 2$ describe the attenuation of the red and blue-green spectra, and K_n describe various constituents in the water, i.e., phytoplankton, detritus, DOC and SPM. For the former three, concentrations of which are explicitly modelled, $K_n = k_n \cdot C_n$, where C_n is the concentration of constituent n, and k_n is the specific attenuation coefficients, which are set to $k_{p_i^C} = 0.015$, $k_{det^C} = 0.01$ and $k_{DOC} = 0.002$ m^2 mmolC[1] (Oubelkheir et al., 2005; Stedmon et al., 2001). For describing the contribution of SPM, K_{SPM}, which is not explicitly modeled here, we use an analytical function of the form:

$$K_{SPM} = K'_{SPM} \cdot f_{SPM}(z) \cdot f_{SPM}(t) \tag{B63}$$

where, the K'_{SPM} is the maximum potential attenuation, $f_{SPM}(z_{max})$ (z_{max}: bottom depth) is a sigmoidal function of depth to account for the cross-shore variations and $f_{SPM}(t)$ (t: day of year) is a sinusoidal function to account for the cyclic seasonal

Table B9. Process equations and functional relationships used in the abiotic module.

O2 O_2 switch	SW_{O2}	if $O2 > 0.0 = 1.0$, else $= 0.0$	(B41)
NO3 NO_3 switch	SW_{NO3}	if $DINO3 > 0.0 = 1.0$, else $= 0.0$	(B42)
Remineralization of DOX	DOX_DIX	$= f_{T,abio} \cdot \lambda^X \cdot DOX$	(B43)
Decay of X={C,N,P} in det_S	$det_S^X\_DOX$	$= f_{T,abio} \cdot r_S^X \cdot det_S^X$	(B44)
Decay of of X={C,N,P,Si} in det_L	$det_L^X\_DOX$	$= f_{T,abio} \cdot r_L^X \cdot det_L^X$	(B45)
Nitrification of pelagic NH4 NH_4	$DINH4\_DINO3$	$= SW_{O2} \cdot f_{T,abio} \cdot DINH4 \cdot r_{nit}$	(B46)
Denitrification in water	$DINO3\_N2$	$= 0.5 \cdot (1 - SW_{O2}) \cdot SW_{NO3} \cdot DOC\_DIC \cdot QN_b$	(B47)
O2 O_2 production by p_i	p_i_O2	$= DIC\_p_i^C \cdot 1.0 [molO2/molC]$	(B48)
O2 O_2 consumption by z_j	$O2\_z_j$	$= z_j^C\_DIC \cdot 1.0 [molO2/molC]$	(B49)
O2 O_2 consumption by remin.	$O2\_DOM$	$= SW_{O2} \cdot DOC\_DIC + (1 - SW_{O2}) \cdot (1 - SW_{NO3}) \cdot DOC\_DIC$	(B50)
O2 O_2 consumption by nitrif.	$O2\_DINH4$	$= DINH4\_DINO3 \cdot 2.0 [molO2/molN]$	(B51)
O2 O_2 flux from air	air_O2	$= k(O2_0 - O2)$, k from Wanninkhof (1992), $O2_0$ from UNESCO (1986)	(B52)
Sedimentation of det_S^X	$det_S^X\_BPOX$	$= \omega_{detL}\omega_{detS} \cdot det_S^X$	(B53)
Sedimentation of det_L^X	$det_L^X\_BPOX$	$= \omega_{detS}\omega_{detL} \cdot det_L^X$	(B54)
Benthic X={C,P,Si} remin.	$BPOX\_DIX$	$= br^X \cdot BPOX$	(B55)
Benthic O2 O_2 consumption	$O2\_BPOM$	$= SW_{O2(b)} \cdot BPOC\_DIC + (1 - SW_{O2(b)}) \cdot (1 - SW_{NO3(b)}) \cdot BPOC\_DIC$	(B56)
Potential benthic denit.	$BPON\_N2'$	$= \rho_{Seitz} \cdot O2\_BPOM$	(B57)
Benthic denitrification	$BPON\_N2$	$= BPON\_N2' - \max(0.0, BPON\_N2' - BPON\_DINH4')$	(B58)
Potential benthic N remin.	$BPON\_DINH4'$	$= br^N \cdot BPON$	(B59)
Benthic N remineralization	$BPON\_DINH4$	$= \max(0.0, BPON\_DINH4' - BPON\_N2')$	(B60)
Benthic NO3 NO_3 reduction	$DINO3\_BPOM$	$= 0.5 \cdot SW_{O2} \cdot SW_{NO3} \cdot BPON\_DINH4$	(B61)

variations driven by the riverine discharges at the coastal region and thermal stratification offshore:

$$630 \quad f_{SPM}(z_{max}) \quad = \quad fz_{minfr} + (1.0 - fz_{minfr}) * (1.0 - 1.0/(1.0 + \exp(z*_{max} - z_{max} * 0.5))) \tag{B64}$$

$$f_{SPM}(t) \quad = \quad F * (A * sin(2.0 \cdot t \cdot \pi/365.0 + 2.0 \cdot L \cdot \pi/365.0) + B) \tag{B65}$$

Based on an analysis (see Kerimoglu, 2014) of the temporally and spatially variable SPM data collected by a Scanfish device (see Maerz et al. (2016) for a description of the data set), and the model performance, we fitted $K'_{SPM} = 1.5$, $fz_{minfr} = 0.3$, $z*_{max} = 7.5$ and $F = 0.05$, $A = 6.0$, $B = 12.0$, $L = 85.0$ for $f_{SPM}(t)$. Finally, for the parameterization of a, η_1 and η_2, we specify the Jerlov Type-1 option in GETM , which corresponds to clear ocean waters (Paulson and Simpson, 1977), given that we explicitly take the attenuation by organic and SPM constituents into account.

References

Ahmerkamp, S., Winter, C., Krämer, K., de Beer, D., Janssen, F., Friedrich, J., Kuypers, M. M., and Holtappels, M.: Regulation of benthic oxygen fluxes in permeable sediments of the coastal ocean, Limnology and Oceanography, 62, 1935–1954, https://doi.org/10.1002/lno.10544, 2017.

Amann, T., Weiss, A., and Hartmann, J.: Carbon dynamics in the freshwater part of the Elbe estuary, Germany: Implications of improving water quality, Estuarine, Coastal and Shelf Science, 107, 112–121, https://doi.org/10.1016/j.ecss.2012.05.012, 2012.

Androsov, A., Fofonova, V., Kuznetsov, I., Danilov, S., Rakowsky, N., Harig, S., Brix, H., and Wiltshire, K. H.: FESOM-C : coastal dynamics on hybrid unstructured meshes, Geoscientific Model Development, 12, 1009–1028, https://doi.org/10.5194/gmd-2018-112, 2019.

Backhaus, J. O.: A three-dimensional model for the simulation of shelf sea dynamics, Deutsche Hydrographische Zeitschrift, 38, 165–187, https://doi.org/10.1007/BF02328975, 1985.

Barthel, K., Daewel, U., Pushpadas, D., Schrum, C., Årthun, M., and Wehde, H.: Resolving frontal structures: on the payoff using a less diffusive but computationally more expensive advection scheme, Ocean Dynamics, 62, 1457–1470, https://doi.org/10.1007/s10236-012-0578-9, 2012.

Becker, E. and Burkhardt, U.: Nonlinear Horizontal Diffusion for GCMs, Monthly Weather Review, 135, 1439–1454, https://doi.org/10.1175/MWR3348.1, 2007.

Becker, G., Dick, S., and Dippner, J.: Hydrography of the German Bight, Marine Ecology Progress Series, 91, 9–18, 1992.

Beckers, J.-M., Burchard, H., Deleersnijder, E., and Mathieu, P.: Numerical Discretization of Rotated Diffusion Operators in Ocean Models, Monthly Weather Review, 128, 2711–2733, 2000.

Beniston, M., Stephenson, D. B., Christensen, O. B., Ferro, C. a. T., Frei, C., Goyette, S., Halsnaes, K., Holt, T., Jylhä, K., Koffi, B., Palutikof, J., Schöll, R., Semmler, T., and Woth, K.: Future extreme events in European climate: an exploration of regional climate model projections, Climatic Change, 81, 71–95, https://doi.org/10.1007/s10584-006-9226-z, 2007.

Blackford, J. C. and Radford, P. J.: A structure and methodology for marine ecosystem modelling, Netherlands Journal of Sea Research, 33, 247–260, https://doi.org/10.1016/0077-7579(95)90048-9, 1995.

Breitbach, G., Krasemann, H., Behr, D., Beringer, S., Lange, U., and Vo, N.: Accessing diverse data comprehensively – CODM , the COSYNA data portal, Ocean Science, 12, 909–923, https://doi.org/10.17616/R3K02T, 2016.

Bruggeman, J. and Bolding, K.: A general framework for aquatic biogeochemical models, Environmental Modelling & Software, 61, 249–265, https://doi.org/10.1016/j.envsoft.2014.04.002, 2014.

Burchard, H. and Badewien, T. H.: Thermohaline residual circulation of the Wadden Sea, Ocean Dynamics, 65, 1717–1730, https://doi.org/10.1007/s10236-015-0895-x, 2015.

Burchard, H. and Bolding, K.: GETM: A general estuarine transport model, Tech. rep., Joint Research Centre, Ispra, Italy, 2002.

Burchard, H. and Hetland, R. D.: Quantifying the Contributions of Tidal Straining and Gravitational Circulation to Residual Circulation in Periodically Stratified Tidal Estuaries, Journal of Physical Oceanography, 40, 1243–1262, https://doi.org/10.1175/2010JPO4270.1, 2010.

Burchard, H. and Rennau, H.: Comparative quantification of physically and numerically induced mixing in ocean models, Ocean Modelling, 20, 293–311, https://doi.org/10.1016/j.ocemod.2007.10.003, 2008.

Burchard, H., Flöser, G., Staneva, J. V., Badewien, T. H., and Riethmüller, R.: Impact of Density Gradients on Net Sediment Transport into the Wadden Sea, Journal of Physical Oceanography, 38, 566–587, https://doi.org/10.1175/2007JPO3796.1, 2008.

Burchard, H., Schuttelaars, H. M., and Ralston, D. K.: Sediment Trapping in Estuaries, Annual Review of Marine Science, 10, 371–395,
690   https://doi.org/10.1146/annurev-marine-010816-060535, 2018.

Burson, A., Stomp, M., Akil, L., Brussaard, C. P. D., and Huisman, J.: Unbalanced reduction of nutrient loads has created an offshore gradient
    from phosphorus to nitrogen limitation in the North Sea, Limnology and Oceanography, 61, 869–888, https://doi.org/10.1002/lno.10257,
    2016.

Callies, U. and Scharfe, M.: Mean spring conditions at Helgoland Roads, North Sea: Graphical modeling of the influence of hydro-climatic
695   forcing and Elbe River discharge, Journal of Sea Research, 101, 1–11, https://doi.org/10.1016/j.seares.2014.06.008, 2015.

Callies, U., Gaslikova, L., Kapitza, H., and Scharfe, M.: German Bight residual current variability on a daily basis: principal components of
    multi-decadal barotropic simulations, Tech. rep., https://doi.org/10.1007/s00367-016-0466-2, 2016.

Callies, U., Gaslikova, L., Kapitza, H., and Scharfe, M.: German Bight residual current variability on a daily basis: principal components of
    multi-decadal barotropic simulations, Geo-Marine Letters, 37, 151–162, https://doi.org/10.1007/s00367-016-0466-2, 2017.

700 Carpenter, J. R., Merckelbach, L., Callies, U., Clark, S., Gaslikova, L., and Baschek, B.: Potential Impacts of Offshore Wind Farms on North
    Sea Stratification, PloS one, 11, e0160 830, https://doi.org/10.1594/WDCC/coastDat-2, 2016.

Chegini, F., Holtermann, P., Kerimoglu, O., Becker, M., Kreus, M., Klingbeil, K., Gräwe, U., Winter, C., and Burchard, H.: Processes of
    stratification and de-stratification during an extreme river discharge event in the German Bight in a model study, Journal of Geophysical
    Research : Oceans.

705 Clark, N., Eber, L., Laurs, R., Renner, J., and Saur, J.: Heat exchange between ocean and atmosphere in the Eastern North Pacific for
    1961–1971, Tech. rep., NOAA, Washington, DC, USA, 1974.

Cloern, J. E., Foster, S. Q., and Kleckner, A. E.: Phytoplankton primary production in the world's estuarine-coastal ecosystems, Biogeo-
    sciences, 11, 2477–2501, https://doi.org/10.5194/bg-11-2477-2014, 2014.

Daewel, U., Schrum, C., and Macdonald, J. I.: Towards end-to-end (E2E) modelling in a consistent NPZD-F modelling framework (ECOSMO
710   E2E_v1.0): application to the North Sea and Baltic Sea, Geoscientific Model Development, 12, 1765–1789, 2019.

Dippner, J. W.: A frontal-resolving model for the German Bight, Continental Shelf Research, 13, 49–66, 1993.

Dolch, T., Buschbaum, C., and Reise, K.: Persisting intertidal seagrass beds in the northern Wadden Sea since the 1930s, Journal of Sea
    Research, 82, 134–141, https://doi.org/10.1016/j.seares.2012.04.007, http://dx.doi.org/10.1016/j.seares.2012.04.007, 2013.

Emeis, K. C., van Beusekom, J., Callies, U., Ebinghaus, R., Kannen, A., Kraus, G., Kröncke, I., Lenhart, H., Lorkowski, I., Matthias, V.,
715   Möllmann, C., Pätsch, J., Scharfe, M., Thomas, H., Weisse, R., and Zorita, E.: The North Sea - A shelf sea in the Anthropocene, Journal
    of Marine Systems, 141, 18–33, https://doi.org/10.1016/j.jmarsys.2014.03.012, 2015.

Fasham, M., Ducklow, H., and Mckelvie, S.: A nitrogen-based model of plankton dynamics in the oceanic mixed layer, Journal of Marine
    Research', 48, 591–639, 1990.

Feng, Y., Friedrichs, M. A., Wilkin, J., Tian, H., Yang, Q., Hofmann, E. E., Wiggert, J. D., and Hood, R. R.: Chesapeake Bay nitrogen fluxes
720   derived from a land-estuarine ocean biogeochemical modeling system: Model description, evaluation, and nitrogen budgets, Journal of
    Geophysical Research G: Biogeosciences, 120, 1666–1695, https://doi.org/10.1002/2015JG002931, 2015.

Fennel, K. and Laurent, A.: N and P as ultimate and proximate limiting nutrients in the northern Gulf of Mexico: Implications for hypoxia
    reduction strategies, Biogeosciences, 15, 3121–3131, https://doi.org/10.5194/bg-15-3121-2018, 2018.

Fennel, K. and Testa, J. M.: Biogeochemical Controls on Coastal Hypoxia, Annual Review of Marine Science, 11, 4.1–4.26,
725   https://doi.org/10.1146/annurev-marine-010318-095138, 2019.

Flöser, G., Burchard, H., and Riethmüller, R.: Observational evidence for estuarine circulation in the German Wadden Sea, Continental Shelf Research, 31, 1633–1639, https://doi.org/http://dx.doi.org/10.1016/j.csr.2011.03.014, 2011.

Flynn, K. J.: Modelling multi-nutrient interactions in phytoplankton; balancing simplicity and realism, Progress in Oceanography, 56, 249–279, https://doi.org/10.1016/S0079-6611(03)00006-5, 2003.

Ford, D. A., van der Molen, J., Hyder, K., Bacon, J., Barciela, R., Creach, V., McEwan, R., Ruardij, P., and Forster, R.: Observing and modelling phytoplankton community structure in the North Sea: can ERSEM-type models simulate biodiversity?, Biogeosciences, 14, 1419–1444, https://doi.org/10.5194/bg-2016-304, http://www.biogeosciences-discuss.net/bg-2016-304/, 2017.

Frey, H.: Stratification during periods of oxygen deficiency in the German Bight during the summers from 1981 to 1983: a comparison with the long-term variation in stratification., Meeresforschung, 32, 306–328, 1990.

Garnier, J., Riou, P., Gendre, R. L., Ramarson, A., Billen, G., Cugier, P., Shapira, M., Théry, S., Thieu, V., and Alain, M.: Managing the Agri-Food System of Watersheds to Combat Coastal Eutrophication: A Land-to-Sea Modelling Approach to the French Coastal English Channel, Geosciences, 9, https://doi.org/10.3390/geosciences9100441, 2019.

Gaslikova, L. and Weisse, R.: coastDat-2 TRIM-NP-2d Tide-Surge North Sea, Tech. rep., WDCC at DKRZ, https://doi.org/10.1594/WDCC/coastDat-2_TRIM-NP-2d, 2013.

Gayer, G., Dick, S., Pleskachevsky, A., and Rosenthal, W.: Numerical modeling of suspended matter transport in the North Sea, Ocean Dynamics, 56, 62–77, https://doi.org/10.1007/s10236-006-0070-5, 2006.

Geider, R., MacIntyre, H., and Kana, T.: Dynamic model of phytoplankton growth and acclimation: responses of the balanced growth rate and the chlorophyll a:carbon ratio to light, nutrient-limitation and temperature, Marine Ecology Progress Series, 148, 187–200, 1997.

Geider, R., Maclntyre, H., and Kana, T.: A dynamic regulatory model of phytoplanktonic acclimation to light, nutrients, and temperature, Limnol. Oceanogr., 43, 679–694, 1998.

Gent, P. R. and McWilliams, J. C.: Isopycnal mixing in ocean circulation models, Journal of Physical Oceanography, 20, 150–155, 1990.

Geyer, B.: High-resolution atmospheric reconstruction for Europe 1948–2012: coastDat2, Earth System Science Data, 6, 147–164, https://doi.org/doi:10.5194/essd-6-147-2014, 2014.

Geyer, W. R. and Maccready, P.: The Estuarine Circulation, Annual Review of Fluid Mechanics, 46, 175–197, https://doi.org/10.1146/annurev-fluid-010313-141302, 2014.

Gräwe, U., Flöser, G., Gerkema, T., Duran-Matute, M., Badewien, T., Schulz, E., and Burchard, H.: A numerical model for the entire Wadden Sea: skill assessment and analysis of hydrodynamics, Journal of Geophysical Research: Oceans, 121, 5231–2551, https://doi.org/10.1002/2016JC011655, 2016.

Griffies, S. M. and Hallberg, R. W.: Biharmonic Friction with a Smagorinsky-Like Viscosity for Use in Large-Scale Eddy-Permitting Ocean Models, Monthly Weather Review, 128, 2935–2946, 2000.

Große, F., Greenwood, N., Kreus, M., Lenhart, H. J., Machoczek, D., Pätsch, J., Salt, L. A., and Thomas, H.: Looking beyond stratification: a model-based analysis of the biological drivers of oxygen deficiency in the North Sea, Biogeosciences, 13, 2511–2535, https://doi.org/10.5194/bgd-12-12543-2015, 2016.

Große, F., Kreus, M., Lenhart, H.-J., Pätsch, J., and Pohlmann, T.: A Novel Modeling Approach to Quantify the Influence of Nitrogen Inputs on the Oxygen Dynamics of the North Sea, Frontiers in Marine Science, 4, 1–21, https://doi.org/10.3389/fmars.2017.00383, 2017.

Grover, J.: Stoichiometry, Herbivory and Competition for Nutrients: Simple Models based on Planktonic Ecosystems, J. Theoret. Biol., 214, 599–618, https://doi.org/10.1006/jtbi.2001.2488, 2002.

Grunwald, M., Dellwig, O., Kohlmeier, C., Kowalski, N., Beck, M., Badewien, T. H., Kotzur, S., Liebezeit, G., and Brumsack, H.-J.: Nutrient dynamics in a back barrier tidal basin of the Southern North Sea: Time-series, model simulations, and budget estimates, Journal of Sea Research, 64, 199–212, https://doi.org/10.1016/j.seares.2010.02.008, http://linkinghub.elsevier.com/retrieve/pii/S1385110110000316, 2010.

Hansen, P., Bjørnsen, P., and Hansen, B.: Zooplankton grazing and growth: Scaling within the 2-2,000˜/mu m body size range, Limnology and Oceanography, 42, 687–704, 1997.

Hickel, W., Mangelsdorf, P., and Berg, J.: The human impact in the German Bight: Eutrophication during three decades (1962-1991), Helgoländer Meeresuntersuchungen, 47, 243–263, https://doi.org/10.1007/BF02367167, 1993.

Hickey, B. M., Kudela, R. M., Nash, J. D., Bruland, K. W., Peterson, W. T., MacCready, P., Lessard, E. J., Jay, D. a., Banas, N. S., Baptista, a. M., Dever, E. P., Kosro, P. M., Kilcher, L. K., Horner-Devine, a. R., Zaron, E. D., McCabe, R. M., Peterson, J. O., Orton, P. M., Pan, J., and Lohan, M. C.: River Influences on Shelf Ecosystems: Introduction and synthesis, Journal of Geophysical Research, 115, C00B17, https://doi.org/10.1029/2009JC005452, 2010.

Hofmeister, R., Beckers, J.-M., and Burchard, H.: Realistic modelling of the exceptional inflows into the central Baltic Sea in 2003 using terrain-following coordinates, Ocean Modelling, 39, 233–247, https://doi.org/10.1016/j.ocemod.2011.04.007, 2011.

Hofmeister, R., Flöser, G., and Schartau, M.: Estuary-type circulation as a factor sustaining horizontal nutrient gradients in freshwater-influenced coastal systems, Geo-Marine Letters, 37, 179–192, https://doi.org/10.1007/s00367-016-0469-z, 2017.

Holt, J. T. and James, I. D.: An assessment of the fine-scale eddies in a high-resolution model of the shelf seas west of Great Britain, Ocean Modelling, 13, 271–291, https://doi.org/10.1016/j.ocemod.2006.02.005, 2006.

Irby, I. D., Friedrichs, M. A., Da, F., and Hinson, K. E.: The competing impacts of climate change and nutrient reductions on dissolved oxygen in Chesapeake Bay, Biogeosciences, 15, 2649–2668, https://doi.org/10.5194/bg-15-2649-2018, 2018.

Izett, J. G. and Fennel, K.: Estimating the Cross-Shelf Export of Riverine Materials: Part 2. Estimates of Global Freshwater and Nutrient Export, Global Biogeochemical Cycles, 32, 176–186, https://doi.org/10.1002/2017GB005668, 2018.

Kantha, L. H. and Clayson, C. A.: Numerical models of oceans and oceanic processes, Academic Press, 2000.

Kerimoglu, O.: Parameterization of turbidity in the German Bight, Tech. rep., Helmholtz-Zentrum Geesthacht, Geesthacht, https://www.hzg.de/imperia/md/content/hzg/zentrale{_}einrichtungen/bibliothek/berichte/hzg{_}reports{_}2019/hzg{_}report{_}2019{_}2.pdf, 2014.

Kerimoglu, O., Hofmeister, R., Maerz, J., Riethmüller, R., and Wirtz, K. W.: The acclimative biogeochemical model of the southern North Sea, Biogeosciences, 14, 4499–4531, https://doi.org/10.5194/bg-14-4499-2017, 2017a.

Kerimoglu, O., Jacquet, S., Vinçon-Leite, B., Lemaire, B. J., Rimet, F., Soulignac, F., Trévisan, D., and Anneville, O.: Modelling the plankton groups of the deep, peri-alpine Lake Bourget, Ecological Modelling, 359, 415–433, https://doi.org/10.1016/j.ecolmodel.2017.06.005, 2017b.

Kerimoglu, O., Große, F., Kreus, M., Lenhart, H.-J., and van Beusekom, J. E.: A model-based projection of historical state of a coastal ecosystem: relevance of phytoplankton stoichiometry, Science of the Total Environment, 639, 1311–1323, https://doi.org/10.1016/j.scitotenv.2018.05.215, 2018.

Klingbeil, K., Mohammadi-Aragh, M., Gräwe, U., and Burchard, H.: Quantification of spurious dissipation and mixing – Discrete variance decay in a Finite-Volume framework, Ocean Modelling, 81, 49–64, https://doi.org/10.1016/j.ocemod.2014.06.001, 2014.

Kondo, J.: Air-sea bulk transfer coefficients in diabatic conditions, Boundary Layer Meteorology, 9, 91–112, 1975.

Laurent, A., Fennel, K., Cai, W.-J., Huang, W.-J., Barbero, L., and Wanninkhof, R.: Eutrophication-induced acidification of coastal waters in the northern Gulf of Mexico: Insights into origin and processes from a coupled physical- biogeochemical model Arnaud, Geophysical Research Letters, 44, 946–956, https://doi.org/10.1002/2016GL071881, 2017.

Lenhart, H., Radach, G., and Ruardij, P.: The effects of river input on the ecosystem dynamics in the continental coastal zone of the North Sea using ERSEM, Journal of Sea Research, 38, 249–274, 1997.

Leote, C., Mulder, L. L., Philippart, C. J. M., and Epping, E. H. G.: Nutrients in the Western Wadden Sea: Freshwater Input Versus Internal Recycling, Estuaries and Coasts, https://doi.org/10.1007/s12237-015-9979-6, http://link.springer.com/10.1007/s12237-015-9979-6, 2015.

805 Löder, M., Kraberg, A., Aberle, N., Peters, S., and Wiltshire, K.: Dinoflagellates and ciliates at Helgoland Roads, North Sea, Helgoland Marine Research, 66, 11–23, https://doi.org/10.1007/s10152-010-0242-z, 2012.

Loebl, M., Dolch, T., and Beusekom, J. E. E. V.: Annual dynamics of pelagic primary production and respiration in a shallow coastal basin, Journal of Sea Research, 58, 269 – 282, https://doi.org/10.1016/j.seares.2007.06.003, 2007.

Loebl, M., Colijn, F., van Beusekom, J., Baretta-Bekker, J., Lancelot, C., Philippart, C., Rousseau, V., and Wiltshire, K.: Recent pat-
810 terns in potential phytoplankton limitation along the Northwest European continental coast, Journal of Sea Research, 61, 34–43, https://doi.org/10.1016/j.seares.2008.10.002, 2009.

Lorkowski, I., Pätsch, J., Moll, A., and Kühn, W.: Interannual variability of carbon fluxes in the North Sea from 1970 to 2006 - Competing effects of abiotic and biotic drivers on the gas-exchange of CO 2, Estuarine, Coastal and Shelf Science, 100, 38–57, https://doi.org/10.1016/j.ecss.2011.11.037, 2012.

815 Los, F., Villars, M., and Van der Tol, M.: A 3-dimensional primary production model (BLOOM/GEM) and its applica-tions to the (southern) North Sea (coupled physical–chemical–ecological model), Journal of Marine Systems, 74, 259–294, https://doi.org/10.1016/j.jmarsys.2008.01.002, 2008.

Maerz, J., Hofmeister, R., van der Lee, E. M., Gräwe, U., Riethmüller, R., and Wirtz, K. W.: Maximum sinking velocities of suspended particulate matter in a coastal transition zone, Biogeosciences, 13, 4863–4876, https://doi.org/10.5194/bg-13-4863-2016, 2016.

820 Merz, B., Elmer, F., Kunz, M., Mühr, B., Schröter, K., and Uhlemann-Elmer, S.: The extreme flood in June 2013 in Germany, La Houille Blanche, 1, 5–10, https://doi.org/10.1051/lhb/2014001, http://www.shf-lhb.org/10.1051/lhb/2014001, 2014.

Middelburg, J. J.: Reviews and syntheses: To the bottom of carbon processing at the seafloor, Biogeosciences, 15, 413–427, https://doi.org/10.5194/bg-15-413-2018, 2018.

Morel, F.: Kinetics of nutrient uptake and growth in phytoplankton, Journal of Phycology, 23, 137–150, 1987.

825 Nasermoaddeli, M. H., Lemmen, C., Stigge, G., Kerimoglu, O., Burchard, H., Klingbeil, K., Hofmeister, R., Kreus, M., Wirtz, K. W., and Kösters, F.: A model study on the large-scale effect of macrofauna on the suspended sediment concentration in a shallow shelf sea, Estuarine, Coastal and Shelf Science, pp. pp. 1–15, https://doi.org/https://doi.org/10.1016/j.ecss.2017.11.002, 2017.

Nasermoaddeli, M. H., Lemmen, C., Stigge, G., Kerimoglu, O., Burchard, H., Klingbeil, K., Hofmeister, R., Kreus, M., Wirtz, K. W., and Kösters, F.: A model study on the large-scale effect of macrofauna on the suspended sediment concentration in a shallow shelf sea,
830 Estuarine, Coastal and Shelf Science, 211, 62–76, https://doi.org/10.1016/j.ecss.2017.11.002, 2018.

OSPAR: Eutrophication Status of the OSPAR Maritime Area. Third Integrated Report on the Eutrophication Status of the OSPAR Maritime Area Submitted by ICG-EMO, Tech. rep., 2017.

Oubelkheir, K., Sciandra, A., and Babin, M.: Bio-optical and biogeochemical properties of different trophic regimes in oceanic waters, Limnology and Oceanography, 50, 1795–1809, https://doi.org/10.4319/lo.2005.50.6.1795, 2005.

835 Pätsch, J. and Kühn, W.: Nitrogen and carbon cycling in the North Sea and exchange with the North Atlantic—A model study. Part I. Nitrogen budget and fluxes, Continental Shelf Research, 28, 767–787, https://doi.org/10.1016/j.csr.2007.12.013, 2008.

Pätsch, J., Burchard, H., Dieterich, C., Gräwe, U., Gröger, M., Mathis, M., Kapitza, H., Bersch, M., Moll, A., Pohlmann, T., Su, J., Ho-Hagemann, H. T., Schulz, A., Elizalde, A., and Eden, C.: An evaluation of the North Sea circulation in global and regional models relevant for ecosystem simulations, Ocean Modelling, 116, 70–95, https://doi.org/10.1016/j.ocemod.2017.06.005, 2017.

840   Paulson, C. and Simpson, J.: Irradience measurements in the upper ocean, Journal of Physical Oceanography, 7, 952–956, 1977.

Payne, R. E.: Albedo of the Sea Surface, Journal of the Atmospheric Sciences, 29, 959–970, https://doi.org/10.1175/1520-0469(1972)029<0959:AOTSS>2.0.CO;2, 1972.

Pein, J., Eisele, A., Hofmeister, R., Sanders, T., Daewel, U., Stanev, E. V., Beusekom, J. V., Staneva, J., and Schrum, C.: Nitrogen cycling in the Elbe estuary from a joint 3D-modelling and observational perspective, Biogeosciences Discussions, pp. 1–34, 2019.

845   Petersen, W., Schroeder, F., and Bockelmann, F.-D.: FerryBox - Application of continuous water quality observations along transects in the North Sea, Ocean Dynamics, 61, 1541–1554, https://doi.org/10.1007/s10236-011-0445-0, http://link.springer.com/10.1007/s10236-011-0445-0, 2011.

Pietrzak, J.: The Use of TVD Limiters for Forward-in-Time Upstream-Biased Advection Schemes in Ocean Modeling, Monthly Weather Review, 126, 812–830, 1998.

850   Platis, A., Siedersleben, S. K., Bange, J., Lampert, A., Bärfuss, K., Hankers, R., Cañadillas, B., Foreman, R., Schulz-stellenfleth, J., Djath, B., Neumann, T., and Emeis, S.: First in situ evidence of wakes in the far field behind offshore wind farms, Scientific Reports, 8, 2163, https://doi.org/10.1038/s41598-018-20389-y, 2018.

Pohlmann, T.: A meso-scale model of the central and southern North Sea: Consequences of an improved resolution, Continental Shelf Research, 26, 2367–2385, https://doi.org/10.1016/j.csr.2006.06.011, 2006.

855   Radach, G.: Ecosystem Functioning in the German Bight Under Continental Nutrient Inputs by Rivers, Estuaries, 15, 477–496, https://doi.org/10.2307/1352392, 1992.

Radach, G. and Pätsch, J.: Variability of Continental Riverine Freshwater and Nutrient Inputs into the North Sea for the Years 1977 – 2000 and Its Consequences for the Assessment of Eutrophication, Estuaries and Coasts, 30, 66–81, https://doi.org/10.1007/BF02782968, 2007.

Roberts, M. and Marshall, D.: Do We Require Adiabatic Dissipation Schemes in Eddy-Resolving Ocean Models?, Journal of Physical
860   Oceanography, 28, 2050–2063, 1998.

Schrum, C.: Thermohaline stratification and instabilities at tidal mixing fronts: Results of an eddy resolving model for the German Bight, Continental Shelf Research, 17, 689–716, https://doi.org/10.1016/S0278-4343(96)00051-9, 1997.

Seitzinger, S. P. and Giblin, A. E.: Estimating denitrification in North Atlantic continental shelf sediments, Biogeochemistry, 35, 235–260, https://doi.org/10.1007/978-94-009-1776-7_7, 1996.

865   Sharples, J., Middelburg, J., Fennel, K., and Jickells, T.: What proportion of riverine nutrients reaches the open ocean?, Global Biogeochemical Cycles, 31, 39–58, https://doi.org/10.1002/2016GB005483, 2017.

Siegismund, F. and Schrum, C.: Decadal changes in the wind forcing over the North Sea, Climate Research, 18, 39–45, 2001.

Simpson, J., Bos, W., Schirmer, F., Souza, A., Rippeth, T., Jones, S., and Hydes, D.: Periodic stratification in the Rhine ROFI in the North Sea, Oceanologica Acta, 16, 23–32, 1993.

870   Smagorinsky, J.: General circulation experiments with the primitive equations. Part I: The basic experiment, Monthly Weather Review, 91, 99–164, https://doi.org/10.1126/science.27.693.594, 1963.

Smith, V. H. and Schindler, D. W.: Eutrophication science: where do we go from here?, Trends in Ecology & Evolution, 24, 201–207, https://doi.org/10.1016/j.tree.2008.11.009, 2009.

Soetaert, K., Middelburg, J. J., Herman, P. M. J., and Buis, K.: On the coupling of benthic and pelagic biogeochemical models, Earth-Science Reviews, 51, 173–201, 2000.

Stanev, E. V., Jacob, B., and Pein, J.: German Bight estuaries : An inter-comparison on the basis of numerical modeling, Continental Shelf Research, 174, 48–65, https://doi.org/10.1016/j.csr.2019.01.001, https://doi.org/10.1016/j.csr.2019.01.001, 2019.

Staneva, J., Stanev, E., Wolff, J.-O., Badewien, T., Reuter, R., Flemming, B., Bartholomä, A., and Bolding, K.: Hydrodynamics and sediment dynamics in the German Bight. A focus on observations and numerical modelling in the East Frisian Wadden Sea, Continental Shelf Research, 29, 302–319, https://doi.org/10.1016/j.csr.2008.01.006, 2009.

Stedmon, C., Markager, S., and Kaas, H.: The optics of chromophoric dissolved organic matter (CDOM) in the Greenland Sea: An algorithm for differentiation between marine and terrestrially derived organic matter, Limnology and Oceanography, 46, 2087–2093, https://doi.org/10.4319/lo.2001.46.8.2087, 2001.

Stips, A., Bolding, K., Pohlmann, T., and Burchard, H.: Simulating the temporal and spatial dynamics of the North Sea using the new model GETM (general estuarine transport model), Ocean Dynamics, 54, 266–283, https://doi.org/10.1007/s10236-003-0077-0, http://dx.doi.org/10.1007/s10236-003-0077-0, 2004.

Straile, D.: Gross growth efficiencies of protozoan and metazoan zooplankton and their dependence on food concentration, predator-prey weight ratio, and taxonomic group, Limnology and Oceanography, 42, 1375–1385, 1997.

Sündermann, J. and Pohlmann, T.: A brief analysis of North Sea physics, Oceanologia, 53, 663–689, https://doi.org/10.5697/oc.53-3.663, http://linkinghub.elsevier.com/retrieve/pii/S0078323411500193, 2011.

UNESCO: Progress on oceanographic tables and standards 1983–1986: work and recommendations of the UNESCO/SCOR/ICES/IAPSO Joint Panel. Technical Papers in Marine Science, 50., Tech. rep., 1986.

van Aken, H. M.: The onset of seasonal stratification in shelf seas due to differential advection in the presence of a salinity gradient, Continental Shelf Research, 5, 475–485, https://doi.org/10.1016/0278-4343(86)90071-3, 1986.

van Beusekom, J. and Brockmann, U.: Transformation of Phosphorus in the Elbe Estuary, Estuaries, 21, 518–526, 1998.

van Beusekom, J. E., Carstensen, J., Dolch, T., Grage, A., Hofmeister, R., Lenhart, H., Kerimoglu, O., Kolbe, K., Pätsch, J., Rick, J., Rönn, L., and Ruiter, H.: Wadden Sea Eutrophication: Long-Term Trends and Regional Differences, Frontiers in Marine Science, 6, 370, https://doi.org/10.3389/fmars.2019.00370, 2019.

van Leeuwen, S., Tett, P., Mills, D., and Van Der Molen, J.: Stratified and nonstratified areas in the North Sea: Long-term variability and biological and policy implications, Journal of Geophysical Research: Oceans, 120, 4670–4686, https://doi.org/10.1002/2014JC010485, 2015.

van Leeuwen, S. M., van der Molen, J., Ruardij, P., Fernand, L., and Jickells, T.: Modelling the contribution of deep chlorophyll maxima to annual primary production in the North Sea, Biogeochemistry, 113, 137–152, https://doi.org/10.1007/s10533-012-9704-5, 2013.

Voynova, Y. G., Brix, H., Petersen, W., Weigelt-Krenz, S., and Scharfe, M.: Extreme Flood Impact on Estuarine and Coastal Biogeochemistry: the 2013 Elbe Flood, Biogeosciences, 14, 541–557, https://doi.org/10.5194/bg-2016-218, 2017.

Wang, Y.: Importance of subgrid-scale parameterization in numerical simulations of lake circulation, Advances in Water Resources, 26, 277–294, 2003.

Wanninkhof, R.: Relationship between wind speed and gas exchange over the ocean, Journal of Geophysical Research, 97, 7373–7382, https://doi.org/10.1029/92JC00188, 1992.

910   Wetz, M. S. and Yoskowitz, D. W.: An 'extreme' future for estuaries ? Effects of extreme climatic events on estuarine water quality and ecology, Marine Pollution Bulletin, 69, 7–18, https://doi.org/10.1016/j.marpolbul.2013.01.020, http://dx.doi.org/10.1016/j.marpolbul.2013.01.020, 2013.

Wiltshire, K. H., Malzahn, A. M., Wirtz, K., Greve, W., Janisch, S., Mangelsdorf, P., Manly, B. F. J., and Boersma, M.: Resilience of North Sea phytoplankton spring bloom dynamics: An analysis of long-term data at Helgoland Roads, Limnology and Oceanography, 53,
915   1294–1302, https://doi.org/10.4319/lo.2008.53.4.1294, 2008.

Zhang, Y. J., Ye, F., Stanev, E. V., and Grashorn, S.: Seamless cross-scale modeling with SCHISM, Ocean Modelling, 102, 64–81, https://doi.org/10.1016/j.ocemod.2016.05.002, 2016.